ISSN 0280-5316
ISRN LUTFD2/TFRT--5827--SE

Estimation of Vehicle Lateral Velocity

Pierre Pettersson

Department of Automatic Control
Lund University
November 2008

Lund University
Department of Automatic Control
Box 118
SE-221 00 Lund Sweden

Document name
MASTER THESIS

Date of issue
November 2008

Document Number
ISRN LUTFD2/TFRT--5827--SE

Author(s)
Pierre Pettersson

Supervisor
Christian Rylander at Halderx, Landskrona
Anders Rantzer Automatic Control (Examiner)

Sponsoring organization

Title and subtitle
Estimation of Vehicle Lateral Velocity (Estimering av ett fordons lateralhastighet)

Abstract
For the performance of the Haldex Active Yaw Control, accurate information about vehicle's lateral dynamic is important. It is for practical reasons not possible to measure the vehicle's lateral velocity, wherefore this state has to be estimated. Previous work [1] with an observer based on a single track bicycle model show promising results but with limited accuracy at high lateral acceleration, therefore was the approach in this thesis to expand the single track model into a two track model to at a more extensive level capture the chassis dynamics. An alternative tire model was developed, because the well known Magic Formula was for this application too computational expensive and the alternative, Exponential tire model, which was previously used in [1] have several disadvantages.
Two observers have been evaluated, the Extended Kalman Filter (EKF) and an Averaging Observer. The EKF is a well known observer that is able to perform well but with the disadvantage to require much calculation power. The Averaging Observer is on the other hand light on calculations, which in this application are desired. Therefore it is tested how well the Averaging Observer performs compared to the EKF. The evaluation was done by comparing the estimated states with the states from both a more complex vehicle model and also real world measurements. The observers performed well in both the cases. The EKF and the Averaging Observer performed almost similar results, which is a favor for the Averaging Observer to achieve same accuracy with less computational effort. Brief tests to do road friction estimations were done and showed promising results if the lateral acceleration sensor signal is reliable.

Keywords

Classification system and/or index terms (if any)

Supplementary bibliographical information

ISSN and key title
0280-5316

ISBN

Language
English

Number of pages
47

Recipient's notes

Security classification

The value of an idea lies in the using of it.

Thomas A. Edison

Preface

This thesis has been done in cooperation with Haldex Traction AB in Landskrona and the department of Control Theory at Lund University.

There are several people whom I like to thank for their help and support in the work of this thesis. First I would like to thank Haldex and the people at the Haldex Traction group for giving me the opportunity to work in this very exciting field. I specially would like to thank Christian Rylander for all support and advice concerning this thesis. Also I like to thank my examinor Anders Rantzer at the department of Control Theory.

Many thanks go to Claus Führer at the department of Numerical Analysis for advices and help with the not always trivial, equations of motion.
Moreover I like to thank Brad Schofield at the department of Control Theory and Per Lidström at the department of Mechanical Engineering for their expertise and invaluable help.
Finally I would like to thank my friends and family, for their continuous encouragement and support.

Lund, October 08
Pierre Pettersson

Table of Content

1. Introduction

1.1 Background

Today is the safety in cars very important and they include numerous systems to protect the driver and passengers in case of an accident. To avoid accidents in first place it is important that the vehicle handling behavior is good and predictable. The vehicle handling behavior is unfortunately not consistent in every situation and the main reason for this is due to non linearity in tire characteristics.

Therefore there are two kind of handling behaviors, linear and non-linear.
The first, when driving inside the linear region the slip between tire and road is small and the vehicle turns proportional with the steer angle which makes the vehicle behavior easy to predict.
If the slip between tire and road is too big the tire characteristics are non-linear and the controllability is reduced which makes the vehicle handling behavior much harder to predict.

If there is a possibility to maintain good handling behavior and predictability in wider range some accidents could be avoided.
One way to accomplish this is by a vehicle stability system based on brake control (ESP) that adjust the brake force on each tire individually to create a stabilizing yaw moment. Because this stabilization technique is based on braking the speed performance is reduced, instead the stabilization can be attained by adjusting the engine torque distribution.

Haldex Traction AB has developed a torque biasing device called
Haldex Limited Slip Coupling which can quickly adjust the torque balance to optimize traction and stability.

To control the torque balance well, information about the vehicle states is needed. Some of the important states like the wheels angular velocity are possible to measure directly but the important vehicle slip angle is not possible to measure with a practical method.

This can be solved by estimate the immeasurable states with use of a model.
The model “simulates” the real car in real time onboard while driving, and by giving the model same inputs as the real car the optimal goal is that they behave exactly the same. The wanted information can then easily be extracted from the model.
Such accurate model is practically impossible to obtain and will because of the required complexity need very much more calculation power than is available in a normal car.

A more convenient approach is to use a simpler model that uses the available measured signals to constantly correct itself toward the state of the real car. A model of this kind is called an observer. There are different kinds of observers and they differ on how they take benefit of the measurement signals, the most known observer is the Kalman filter.

One of the main objectives with this work was to design such observer to estimate the lateral velocity which is used to calculate vehicle slip angle.

1.2 Related work

In the Master Thesis, **'Design and Validation of a Vehicle State Estimator'** of Schoutissen S.L.G.F. at Haldex Traction 2004, an observer based on a single track bicycle model was proposed to estimate the lateral velocity.

It proved that it is with use of an observer possible to estimate the lateral velocity. Also a road friction coefficient estimator was proposed.

The use of a single track model has the advantage to be simple and still capture most important chassis dynamics.
A main disadvantage is that it doesn't capture the chassis roll dynamics. The chassis roll dynamics affects the load transfer to the different wheels which then affects the tire friction forces that are essential in order to estimate the lateral velocity.

Since the single track model didn't have any roll dynamics the use of the important lateral acceleration sensor was also limited. Because then the chassis is under roll the lateral acceleration sensor gets an offset and scale error because it's no longer parallel with the ground and it will be affected by the gravitation force.
To correctly compensate for this, the chassis roll angle is needed.

1.3 Problem formulation

This work is a renewal of the Master Thesis, **'Design and Validation of a Vehicle State Estimator'** with the ideá that by using a two track model which in difference from the single track model captures the chassis roll dynamics, a more accurate estimation of the lateral velocity is expected.

The tire forces are very important for accurate estimation of the lateral velocity, so it is also desirable to use as good tire model as possible.
To get the tire model to work correctly the friction coefficient μ between tire and road is needed. This friction coefficient changes with road surface, so it is also desirable to be able to change μ over time.
In this work the friction coefficient is assumed to be known.

A second objective is to look into possibilities to use this two track model as a platform for friction coefficient estimation.

The model must not be too complex, because it should be possible to implement in a vehicle, where computation power is much limited.

2. Vehicle Model

2.1 Overview

The vehicle model should capture the vehicle dynamics as good as possible but without be too complex. The model used in this work is a two track model which has five degrees of freedom, longitudinal velocity, lateral velocity, yaw-rate, roll angle and pitch angle.
It's later shown from simulations that the pitch angle can for most cases be neglected and be removed if calculation power is needs to be saved.

The model can primarily be divided into two essential parts, tire model and chassis model. These are coupled in the way that the input for the tire model is the chassis movements and the chassis model has the tire forces as input.

The coordinate systems and sign convention used in the representation of the vehicle's motion are chosen to the ISO standard [2]. The x-axis corresponds to the longitudinal axis, positive in forward direction. The y-axis corresponds to the lateral axis with positive to the left and z-axis corresponds to the axis normal to ground. Rotation around x-axis is called roll (ϕ), rotation around y-axis is called pitch θ and rotation around z-axis is called yaw (ψ). It's for the yaw-rate common to simply use r instead of $\dot{\psi}$, this is avoided in this report to avoid misunderstanding.
The coordinate system is shown in Figure 2.1. Notice that the lateral velocity V_y is negative in the figure, so is also the chassis slip angle β.

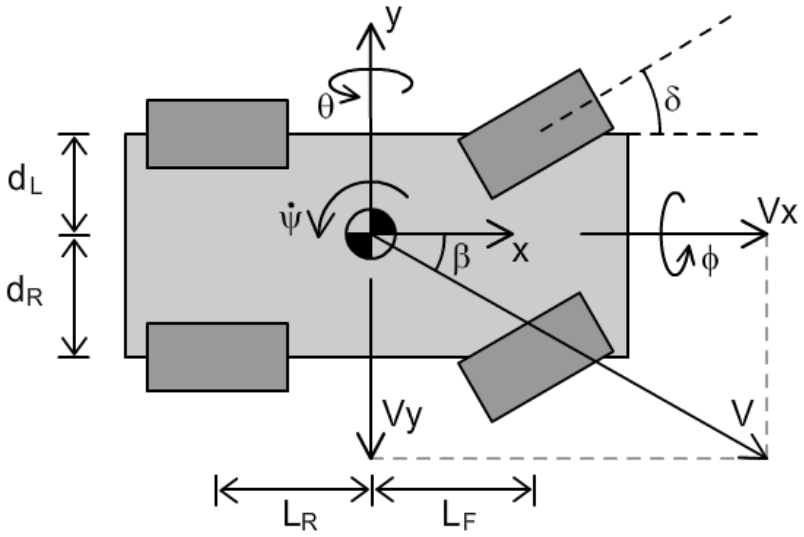

Figure 2.1 – Coordinate system. (V_y and β are negative in the figure)

2.2 Tire Model

The tire is probably the very most difficult part to model correctly. Much research has been done in this field and trough the last decades plentiful of books and papers have been published. Yet there is no tire model which perfect represent a true tire even if there exists very complex models which are close to reality.
In this work the tire model has to be kept simple due to the limited calculation power.

Camber and caster angles are because of their small contribution [2] neglected in order to keep the model simple.

2.2.1 Magic Formula

The Magic Formula tire model is a widely used semi-empirical model which has proven to give good results and also can be made quite light on computations.
The expression for the lateral tire force F_y in pure slip given by the Magic Formula is,

$$F_y = D\sin[C\arctan\{B\alpha - E(B\alpha - \arctan(B\alpha))\}] \qquad (2.1)$$

where:

$B = \frac{C_{F\alpha}}{CD}$ is the stiffness factor

$D = \mu F_z = F_{y,peak}$ is the peak factor

$C_{F\alpha} = c_1 \sin\left(2\arctan\left(\frac{F_z}{c_2}\right)\right)$

C, E are shape factors
c_1 is the maximum cornering stiffness
c_2 is the load at maximum cornering stiffness

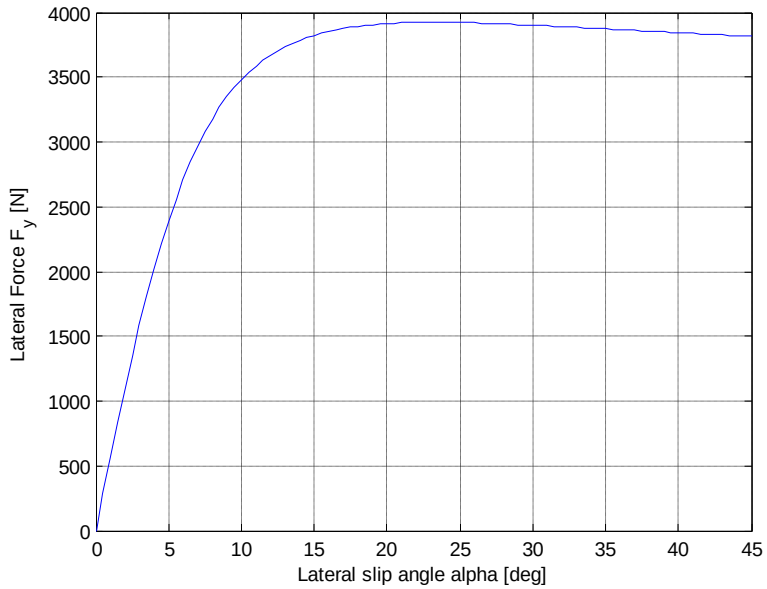

Figure 2.1 – How lateral force F_y given by Magic Formula depends on slip angle α

Despite this simplified form of the Magic Formula it is because with all the inverse tangent functions too heavy to compute at real time in a cars hardware.

2.2.2 Exponential tire model

One simpler model is the Exponential tire model.
In Figure 2.2 one see that the Exponential tire model differs from Magic Formula at e.g. a slip angle of five degrees. If a vehicle stays in this region for some time, piling up errors is quickly introduced in estimation of the lateral velocity, example of this can be found in reference [1]. Because of this, it is desired if possible not to use the Exponential tire model.

2.2.3 Polynomial tire model

Another approach is the idea that the lateral force curve given by Magic Formula could be approximated with a polynomial. To avoid heavy calculations the polynomial should have as low degree as possible. There is however no low degree polynomial that fits on the entirely curve well, although by divide the curve in smaller pieces it is possible. Each piece is given its own unique polynomial approximation.
The polynomial coefficients are pre calculated and chosen such that the root mean square of the error then compared to the Magic Formula is minimized, with extra condition to not have any discontinues (jumps) between pieces.

Such polynomial gives the Lateral force F_y for a given slip angle α but the Lateral force F_y also depends on the Normal force F_z and the friction coefficient μ which both affect the Lateral force non-linear, as seen in equation (2.1).
To handle this, the tire slip angle α is before used in the polynomial modified with a scale factor which depends on the Normal force F_z and the friction coefficient μ.

$$\alpha_{modified} = \alpha \frac{(c_1 F_z^2 + c_2 F_z + c_3)}{\mu}$$

c_1, c_2 and c_3 are tunable parameters. If necessary, it is possible to neglect the term $c_1 F_z^2$ without losing too much accuracy.

As seen in Figure 2.2 and 2.3 the Polynomial tire model correspond very well to the Magic Formula and the highest degree of polynomial in use is of degree two.

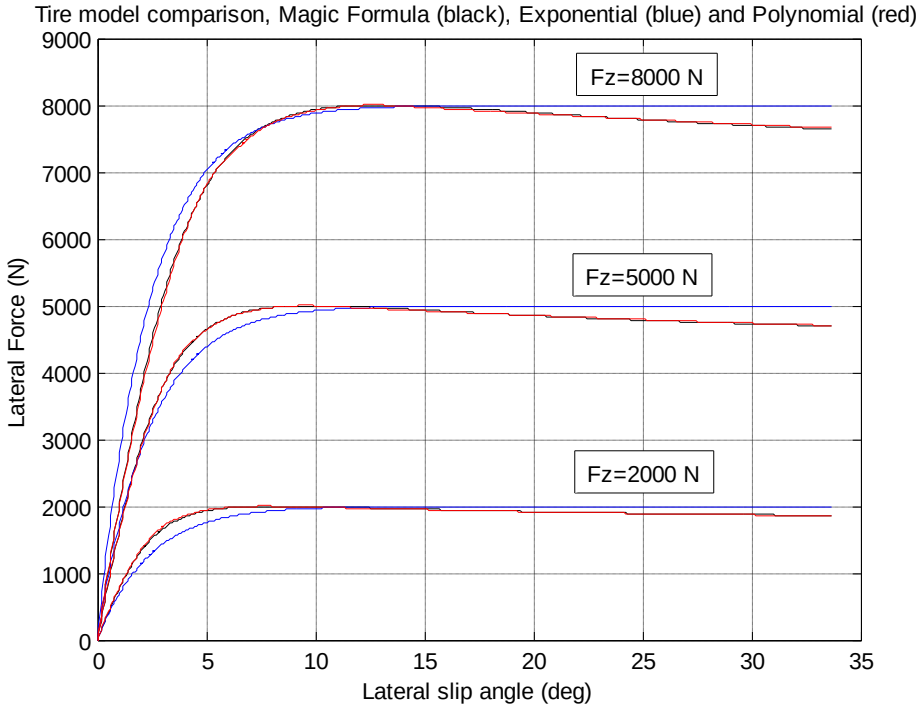

Figure 2.2 – Tire model comparisons with different loads

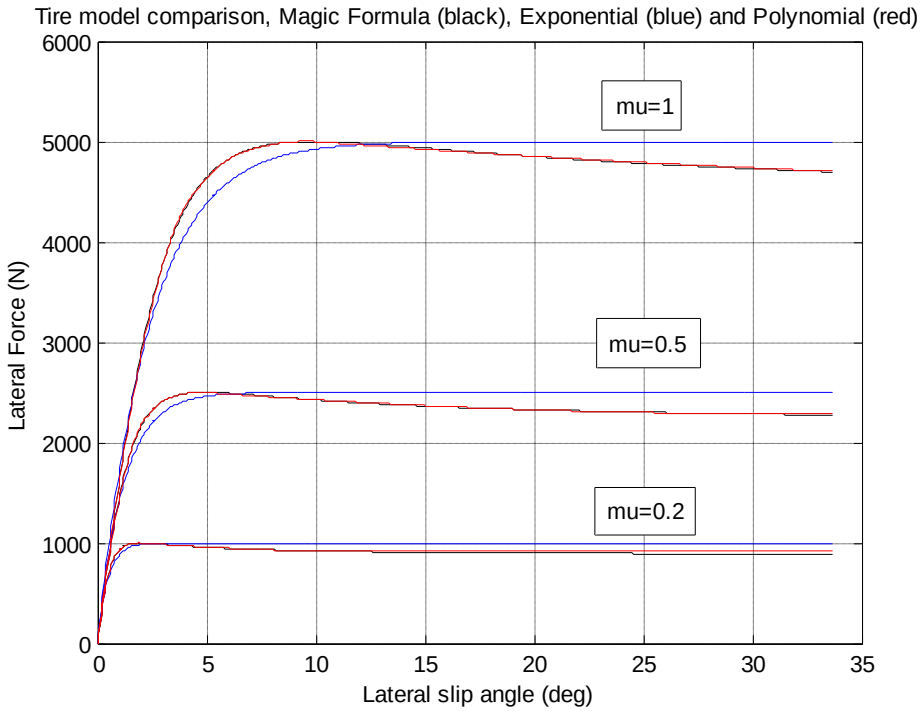

Figure 2.3 – Tire model comparisons with different friction coefficients

In Figure 2.2 and 2.3 it's clear that between the Polynomial and Exponential tire model, the Polynomial tire model gives best results under different slip angles, loads and friction coefficients.

2.2.4 Combined Slip

If the tire is forced by engine- or brake torque to have a circumferential speed different than a free rolling tire, a longitudinal slip is created. Like the lateral slip, the longitudinal slip determines the force created by the tire. The problem that occurs when modeling a tire is that the lateral tire force depends on both the lateral and longitudinal slip, and vice versa, the longitudinal tire force depends on both the longitudinal and lateral slip.
If high accuracy is needed, the tire model that models the correlation between the different slips and forces has to be quite complex, se reference [2] for details.

To save resources, this application is using a rather simplified approach. The idea is that the more the tire slip in longitudinal direction, the less ability has the tire to develop lateral grip.
The procedure is that first the wheel angular speed is measured and multiplied with the tire radii to get the tire velocity, which together with the estimated hub velocity determines the estimated longitudinal slip.
Then the lateral tire force is calculated as normal but with use of a reduced road friction coefficient. The amount the road friction coefficient is reduced is determined by the magnitude of the estimated longitudinal slip.

$$\kappa^i = \frac{v_x^i - \varpi^i R_t}{\left|v_x^i\right|}$$

$$\mu_{lat}^i = \mu - c\left|\kappa^i\right|$$

How much the lateral friction is reduced by the longitudinal slip is not trivial. Tests has shown that a value of $c = 1/4$ works well.
There is also possible to use powers of κ.

2.3 Chassis Model

The chassis model has five degrees of freedom and is a non-linear process, which in discrete time domain can be formulated:

$$x_{t+1} = f(x_t, u_{t+1})$$

x_t is the vehicle state vector at time t and u_t is the input vector.
In f the equation of motion are included and also the numerical integration.

2.3.1 Vehicle states

The used states are:

- Longitudinal velocity - v_x
- Lateral acceleration and velocity - $\dot{v}_y$, v_y
- Yaw rate - $\dot{\psi}$
- Roll angle velocity and position - $\dot{\phi}, \phi$
- Pitch angle velocity and position - $\dot{\theta}, \theta$

Longitudinal velocity
In this work it is assumed that there exists a measurement signal of the longitudinal velocity which then will be used by the observer. A common method to obtain the longitudinal velocity is to use the wheel angular velocity sensors. Because of eventual wheel spin, the signal from the wheel with highest estimated vertical load is weighted most, because this wheel is most likely to have the smallest amount of slip.
The wheels angular velocity is multiplied with the tire radii to get an estimation of the longitudinal velocity. The tire radii can either be a fixed value that is predefined or if a more accurate estimation of the longitudinal velocity is needed the tire is modeled to change radii at different loads.

Lateral acceleration and velocity
Since there is no sensor to measure the lateral velocity, this state is estimated by integrating the estimated lateral velocity change.
Therefore the velocity change rate is required to be estimated accurate in order to avoid piling up errors when integrating.

The lateral acceleration sensor has potential to give fast and accurate measurement of this state value but can be difficult to read off correctly.
In addition to the vehicle lateral velocity change ($\dot{v}_y$) the sensor is also affected by the centripetal force, and if the chassis is under roll the sensor is also affected by the gravity force, Figure 2.4, 2.5.

$$a_y^{sensor} = \left(\dot{v}_y + \frac{F_c}{m} \right) \cos(\phi) + g \sin(\phi) = \left(\dot{v}_y + v_x \dot{\psi} \right) \cos(\phi) + g \sin(\phi)$$

$$F_c = \frac{m v_x^2}{R} = m v_x \frac{v_x}{R} = m v_x \dot{\psi}$$

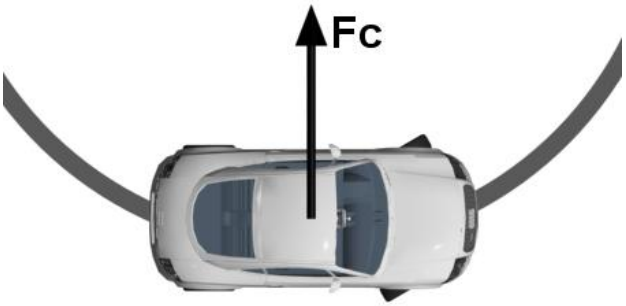

Figure 2.4 – The centripetal force at a turn

The contribution from the centripetal force is often a very large part of the resultant force and is therefore critical to estimate well, this need accurate estimation of yaw-rate and longitudinal velocity.

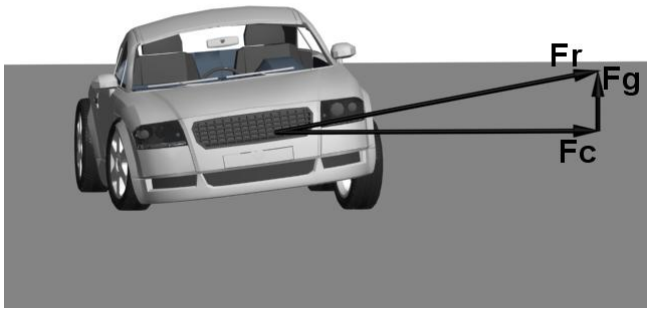

Figure 2.5 – Due to chassis roll the lateral acceleration sensor is affected by the gravity force

Yaw rate
The yaw rate is the time derivative of the yaw angle ψ, Figure 2.6.

A yaw rate sensor, also called gyro-meter, measures the angular velocity of the chassis along its vertical axis.
Accurate information about the yaw rate is for many reasons very important and modern cars have therefore often a yaw-rate sensor.

Yaw-rate can also be estimated by use of measured wheel angular velocities.
This estimation is often less accurate than the yaw-rate sensor signal but by combining them both in a Kalman filter or a recursive least square algorithm it is possible to achieve higher accuracy than by only using the yaw-rate sensor.
However, this method has a drawback because if engine or break torque is applied the wheel angular velocities may lose information about the yaw-rate.

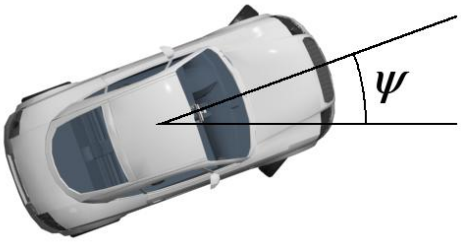

Figure 2.6 – Yaw angle

Roll angle acceleration, velocity and position
When the vehicle enters a turn the chassis will roll. This is important to estimate because the roll angle position tells how much the springs are compressed and the roll angle velocity (roll rate) tells how much the dampers are affected. This gives the load transfer and tire normal forces which are used by the tire model.

As written before, the roll angle also needed to compensate the lateral acceleration sensor.

The roll is not possible to measure, and very few vehicles are equipped with a roll rate sensor, so the estimation has to entirely be based on the model.

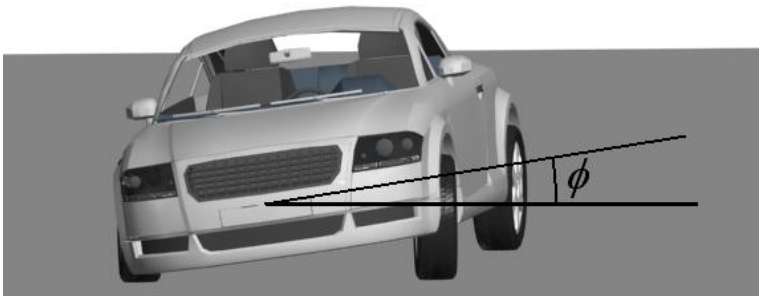

Figure 2.7 – Chassis roll angle

Pitch angle velocity and position
If the vehicle changes its longitudinal velocity the chassis will pitch. By the same reasons as for the roll angle, the pitch angle will affect the load transfer which is used by the tire model.

Nor the pitch angle is possible to measure so the estimation has to entirely rely on the model.

Figure 2.8 – Chassis pitch angle

2.3.2 Equations of motion

The equations of motion follow Newton's second law and can be written:

$$M\ddot{X} = F$$

F is the force and momentum vector.

$$F = \begin{bmatrix} T \\ R - \varpi \times (I_{RR}\varpi) \end{bmatrix}$$

T and *R* are the external force and momentum vectors, I_{RR} is the inertia matrix and ϖ is the angular velocity vector. Despite the name is the angular velocity vector (ϖ) not simply the vector with the angular velocities, because when rotating along several axles, the rotation of one axle affects the rotation direction of another axle. Therefore does ϖ in the three dimensional case grow in complexity.

$$\varpi = G\begin{bmatrix} \dot{\phi} \\ \dot{\theta} \\ \dot{\psi} \end{bmatrix} = \begin{bmatrix} \dot{\phi} - \dot{\psi}\sin(\theta) \\ \dot{\theta}\cos(\phi) + \dot{\psi}\sin(\phi)\cos(\theta) \\ \dot{\psi}\cos(\phi)\cos(\theta) - \dot{\theta}\sin(\phi) \end{bmatrix}$$

$$G = \begin{bmatrix} 1 & 0 & -\sin(\theta) \\ 0 & \cos(\phi) & \sin(\phi)\cos(\theta) \\ 0 & -\sin(\phi) & \cos(\phi)\cos(\theta) \end{bmatrix}$$

$$T = \begin{bmatrix} F_x \\ F_y \\ F_z \end{bmatrix} = \begin{bmatrix} F_{Tx} + mv_y\dot{\psi} \\ F_{Ty} - mv_x\dot{\psi} \\ F_{Tz} - mg \end{bmatrix}, \quad R = \begin{bmatrix} M_x \\ M_y \\ M_z \end{bmatrix}$$

The external forces and momentums are functions of the tire forces.

$$F_{Tx} = F_{RLx} + F_{RRx} + (F_{FLx} + F_{FRx})\cos(\delta) - (F_{FLy} + F_{FRy})\sin(\delta)$$
$$F_{Ty} = F_{RLy} + F_{RRy} + (F_{FLy} + F_{FRy})\cos(\delta) + (F_{FLx} + F_{FRx})\sin(\delta)$$
$$F_{Tz} = F_{FLz} + F_{FRz} + F_{RLz} + F_{RRz}$$

$$M_x = d_L \cdot F_{FLz} + d_R \cdot F_{FRz} + d_L \cdot F_{RLz} - d_R \cdot F_{RRz} + (F_{RLx} + F_{RRx} + (F_{FLy} + F_{FRy})\cos(\delta) + (F_{FLx} + F_{FRx})\sin(\delta))\, h$$

$$M_y = -L_F \cdot F_{FLz} - L_F \cdot F_{FRz} + L_R \cdot F_{RLz} + L_R \cdot F_{RRz} + (-F_{RLx} - F_{RRx} - (F_{FLx} + F_{FRx})\cos(\delta) + (F_{FLy} + F_{FRx})\sin(\delta))\, h$$

$$M_z = (F_{FLx} + F_{FRx})\, L_F \sin(\delta) + (F_{FLy} + F_{FRy})\, L_F \cos(\delta) - (F_{RLy} + F_{RRy})\, L_R + (-F_{FRy}\sin(\delta) + F_{FRx}\cos(\delta) + F_{RRx})\, d_R + (F_{FLy}\sin(\delta) - F_{FLx}\cos(\delta) - F_{RLx})\, d_L$$

The mass matrix *M* contains four 3x3 matrices. M_{TT} is the translation mass matrix and M_{RR} is the rotation inertia matrix.

$$M = \begin{bmatrix} M_{TT} & M_{RT} \\ M_{RT} & M_{RR} \end{bmatrix},\ M_{TT} = m I_{3\times3},\ M_{RR} = G^T I_{RR} G,\ I_{RR} = \begin{bmatrix} I_{xx} & 0 & 0 \\ 0 & I_{yy} & 0 \\ 0 & 0 & I_{zz} \end{bmatrix}$$

The M_{RT} mass matrix is zero if the rotation centre takes place around the centre of gravity.
The offset of the rotation centre affect the structure of the *U* matrix, in this case the offset is only in z-direction because it is the most common displacement of the chassis roll centre.

$$M_{RT} = -AU\,G,\ A = R_x R_y R_z,\ U = \begin{bmatrix} 0 & mh & 0 \\ mh & 0 & 0 \\ 0 & 0 & 0 \end{bmatrix}$$

$$R_x = \begin{bmatrix} 1 & 0 & 0 \\ 0 & \cos(\phi) & -\sin(\phi) \\ 0 & \sin(\phi) & \cos(\phi) \end{bmatrix},\ R_y = \begin{bmatrix} \cos(\theta) & 0 & -\sin(\theta) \\ 0 & 1 & 0 \\ \sin(\theta) & 0 & \cos(\theta) \end{bmatrix},$$
$$R_z = \begin{bmatrix} \cos(\psi) & -\sin(\psi) & 0 \\ \sin(\psi) & \cos(\psi) & 0 \\ 0 & 0 & 1 \end{bmatrix}$$

For a full explanation about these equations it is suggested to read reference [4].

This formulation of the equation of motion is by far too complex for usage in this application, and has somehow to be approximated.
The mass matrix *M* is in this formulation not constant in time and contain off diagonal elements. This makes it necessary to do a costly matrix inversion at each time step.
In this application the angles are expected to be small and it is therefore possible to let both of the matrices *G* and *A* be set to the identity matrix, which makes M_{RT} and M_{RR} constant.
The entire mass matrix *M* is now assumed to be constant and can be pre-inverted offline.
If *G* is assumed to be the identity matrix even then calculating the angular velocity vector the equations shortens dramatically.

Comparison between the original model and the approximation

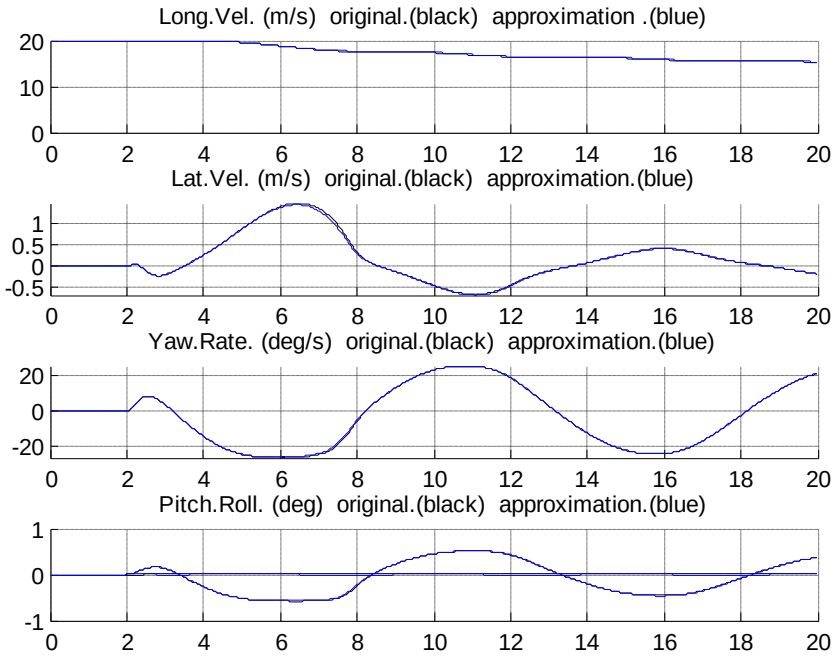

Figure 2.9

At the comparison in Figure 2.9 it is hard to distinguish the approximated model from the original model. The approximation can therefore in this application be used without losing any significant accuracy.

2.4 Damper model

Damper characteristics are in general not linear. In Figure 2.9 an example of a typical damper characteristic is shown. To model this one can use a lookup table and do linear interpolation.
To get a smooth curve this needs a relatively large lookup table and at every time step an interpolation has to take place.
Instead a polynomial approach is used, much like the one used in the tire model.

By using the origin large lookup table, the curve is divided in several parts which are approximated by either a first or second degree polynomial. The break points and polynomial coefficients are chosen to minimize the error. The polynomial coefficients now serve as the look up table.

This method decreases computation time because there is no need at every time step to do an interpolation because the interpolation coefficients are already pre calculated. Memory usage is also decreased because the new lookup table is smaller.

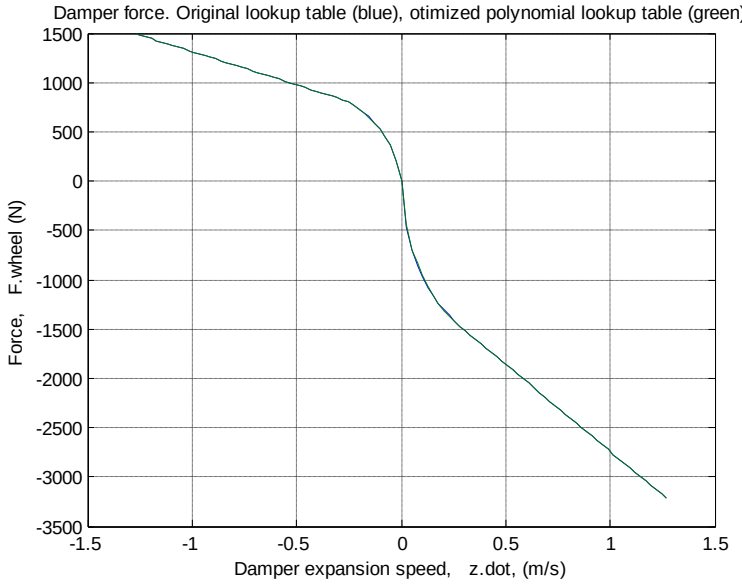

Figure 2.10 – Damper characteristics

2.5 Two track model, step by step

1. Velocity at the corners

The velocity at each wheel hub is determined, based on chassis longitudinal- lateral velocity, yaw-rate and steer angle.

$$L_{FL} = \begin{bmatrix} L_F \\ d_L \\ 0 \end{bmatrix}, L_{FR} = \begin{bmatrix} L_F \\ -d_R \\ 0 \end{bmatrix}, L_{RL} = \begin{bmatrix} -L_R \\ d_L \\ 0 \end{bmatrix}, L_{RR} = \begin{bmatrix} -L_R \\ -d_R \\ 0 \end{bmatrix}, \quad \dot{\Psi} = \begin{bmatrix} 0 \\ 0 \\ \dot{\psi} \end{bmatrix}$$

$$R_\delta = \begin{bmatrix} \cos(\delta) & -\sin(\delta) & 0 \\ \sin(\delta) & \cos(\delta) & 0 \\ 0 & 0 & 1 \end{bmatrix}$$

$$\bar{v}_{FL}^{hub} = \left(v_{CoG} + (\dot{\Psi} \times L_{FL})\right) \cdot R_\delta$$
$$\bar{v}_{FR}^{hub} = \left(v_{CoG} + (\dot{\Psi} \times L_{FR})\right) \cdot R_\delta$$
$$\bar{v}_{RL}^{hub} = v_{CoG} + (\dot{\Psi} \times L_{RL})$$
$$\bar{v}_{RR}^{hub} = v_{CoG} + (\dot{\Psi} \times L_{RR})$$

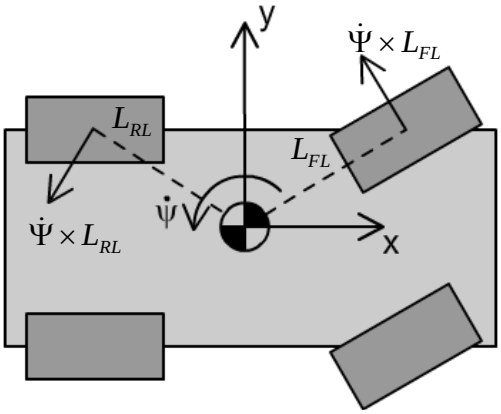

Figure 2.11 – Geometric explanation how the wheel hub velocities are affected by the yaw-rate.

2. Tire normal forces

Because of the eventual load transfer, each tire has a different normal force.
With knowledge of the chassis roll/pitch angles and roll/pitch angle velocities the forces caused by the springs, dampers and anti-roll bar can be determined. To this the force of gravity is also added.

$$z_{FL}^{hub} = -L_F \sin(\theta) + d_L \sin(\phi), \quad \dot{z}_{FL}^{hub} = -L_F \dot{\theta} \cos(\theta) + d_L \dot{\phi} \cos(\phi)$$
$$z_{FR}^{hub} = -L_F \sin(\theta) - d_R \sin(\phi), \quad \dot{z}_{FR}^{hub} = -L_F \dot{\theta} \cos(\theta) - d_R \dot{\phi} \cos(\phi)$$
$$z_{RL}^{hub} = +L_R \sin(\theta) + d_L \sin(\phi), \quad \dot{z}_{RL}^{hub} = +L_R \dot{\theta} \cos(\theta) + d_L \dot{\phi} \cos(\phi)$$
$$z_{RR}^{hub} = +L_R \sin(\theta) - d_R \sin(\phi), \quad \dot{z}_{RR}^{hub} = +L_R \dot{\theta} \cos(\theta) - d_R \dot{\phi} \cos(\phi)$$

$$F_{FLz}^{tire} = g\, m_{FL} - K_{\mathrm{F}}^{spring} \cdot z_{FL}^{hub} - f_F^{damper}(\dot{z}_{FL}^{hubb}) - K_F^{\text{anti roll}}(z_{FL}^{hub} - z_{FR}^{hub})$$
$$F_{FRz}^{tire} = g\, m_{FR} - K_{\mathrm{F}}^{spring} \cdot z_{FR}^{hub} - f_F^{damper}(\dot{z}_{FR}^{hubb}) - K_F^{\text{anti roll}}(z_{FR}^{hub} - z_{FL}^{hub})$$
$$F_{RLz}^{tire} = g\, m_{RL} - K_{\mathrm{R}}^{spring} \cdot z_{RL}^{hub} - f_R^{damper}(\dot{z}_{RL}^{hubb}) - K_R^{\text{anti roll}}(z_{RL}^{hub} - z_{RR}^{hub})$$
$$F_{RRz}^{tire} = g\, m_{RR} - K_{\mathrm{R}}^{spring} \cdot z_{RR}^{hub} - f_R^{damper}(\dot{z}_{RR}^{hubb}) - K_R^{\text{anti roll}}(z_{RR}^{hub} - z_{RL}^{hub})$$

The damper function $f^{damper}(\dot{z}^{hub})$ is explained above at 2.4.

3. Tire longitudinal and lateral forces

With values on the wheel velocity vectors and wheel angular velocities the longitudinal and lateral tire slip values can be determined. Combined with the tire normal forces the lateral and longitudinal tire forces can be determined with use of the tire model.

$$\left[F_x^{tire}, F_y^{tire}\right] = f_{\text{Tire model}}(F_z, v_x^{hub}, v_y^{hub}, \omega)$$

How these forces relate is explained in the section about the tire model at chapter 2.2

4. Summation of forces and momentums

The longitudinal- lateral- and normal tire forces are summed up to resulting lateral and longitudinal forces at the chassis. The tire forces also create momentums around the three rotation axles, pitch, roll and yaw.

$$F_{Tire\ x} = F_{RLx} + F_{RRx} + (F_{FLx} + F_{FRx})\cos(\delta) - (F_{FLy} + F_{FRy})\sin(\delta)$$
$$F_{Tire\ y} = F_{RLy} + F_{RRy} + (F_{FLy} + F_{FRy})\cos(\delta) + (F_{FLx} + F_{FRx})\sin(\delta)$$

$$M_x = d_L \cdot F_{FLz} - d_R \cdot F_{FRz} + d_L \cdot F_{RLz} - d_R \cdot F_{RRz} + F_{Tire\ y}\, h_{RC}$$

$$M_y = -L_F \cdot F_{FLz} - L_F \cdot F_{FRz} + L_R \cdot F_{RLz} + L_R \cdot F_{RRz} + F_{Tire\ x}\, h_{PC}$$

$$M_z = (F_{FLx} + F_{FRx})\, L_F \sin(\delta) + (F_{FLy} + F_{FRy})\, L_F \cos(\delta) - (F_{RLy} + F_{RRy})\, L_R +$$
$$(-F_{FRy}\sin(\delta) + F_{FRx}\cos(\delta) + F_{RRx})\, d_R + (F_{FLy}\sin(\delta) - F_{FLx}\cos(\delta) - F_{RLx})\, d_L$$

5. Acceleration equations

Newton's second law says that acceleration is the applied force divided with the mass, the angular acceleration work analogous with momentum and inertia instead of force and mass.

As explained before in chapter 2.3.2, the equations are expanded because of the chassis roll axis are not intersecting the center of gravity. Also it is showed that most of these extra terms can be neglected due to their minor influence.

It is important to make clear that $\dot{v}_x \neq a_x$ and $\dot{v}_y \neq a_y$.

$$a_x = \frac{F_{Tire\ x}}{m}, \quad a_y = \frac{F_{Tire\ y}}{m}$$

$$\dot{v}_x = a_x + v_y \dot{\psi}, \quad \dot{v}_y = a_y - v_x \dot{\psi}$$

$$\ddot{\phi} = \frac{M_x}{I_{xx}}, \quad \ddot{\theta} = \frac{M_y}{I_{yy}}, \quad \ddot{\psi} = \frac{M_z}{I_{zz}}$$

6. Numerical integration

The final step is to with an appropriate numerical scheme integrate the acceleration equations to obtain the longitudinal- lateral velocity, yaw rate, roll and pitch angles. Common methods are the explicit/implicit Euler method and Tustin, the later also known as the trapezoidal method.

Explicit Euler method: $x_{i+1} = x_i + dt\ \dot{x}_i$

Implicit Euler method: $x_{i+1} = x_i + dt\ \dot{x}_{i+1}$

Tustin: $x_{i+1} = x_i + \frac{dt}{2}(\dot{x}_{i+1} + \dot{x}_i)$

It is important to consider the stability of the numerical integration. The figure below show how a stable continuous-time system maps into a discrete-time system with the three different methods. The unit circle corresponds to the stability region of the discrete system.

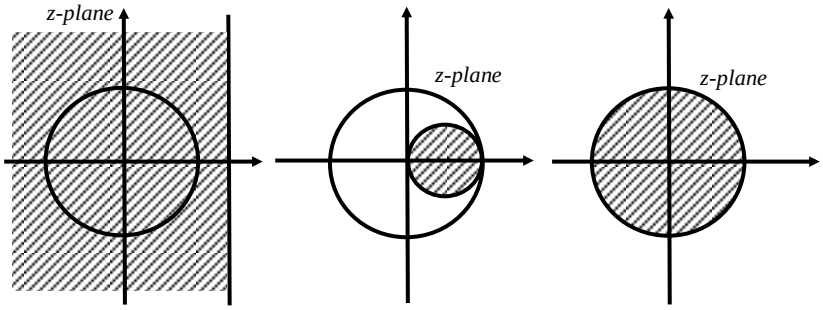

Explicit Euler *Implicit Euler* *Tustin*

The implicit Euler is somewhat too stable. A discretization of an unstable continuous-time system can with this method transform into a stable discrete-time system.
In opposite is the explicit Euler too unstable and there is a chance that a stable continuous-time system transform into an unstable discrete-time system.
The Tustin method preserves the stability region and is therefore commonly used.
Support for these theories and more in deep information can be read in reference [3].

Both the implicit Euler and Tustin are implicit methods and requires a non-linear equation system to be solved, this is too computational costly for this application and the explicit Euler method has to be used.
For improved stability is a symplectic Euler method used in case of the roll and pitch angles. The method can somewhat be described as a semi-implicit method and can with advantage be used then integrating from acceleration to position. It requires no extra work compared to the ordinary explicit Euler method.

$$\dot{\phi}_{i+1} = \dot{\phi}_i + dt\ \ddot{\phi}_i$$

$$\phi_{i+1} = \phi_i + dt\ \dot{\phi}_{i+1}$$

3. Observer Design

3.1 Overview

Because the model is just a model it will not entirely represent the real car. This causes unavoidable errors in predicted states. Drift offs is expected.
To deal with this problem it is possible to use sensors to measure different states of the vehicle and use that information to make corrections on the model. This is what the observer does.
The question is how to use the measurements to correct the model.
Basically one use the simulated states to predict what the sensors will measure, then correct the states so the difference between measurements and predicted measurements are minimized.

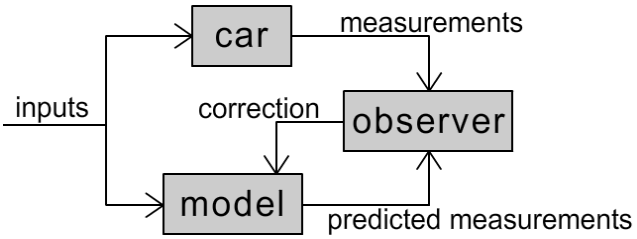

Figure 3.1 – Model and observer interaction

One way to do this is to use a Kalman Filter, which is the most known observer. Because the vehicle model is a non-linear process it is not possible to use the ordinary linear Kalman Filter but there exists an Extended Kalman Filter (EKF) which works at non-linear systems. However the EKF have some major drawbacks. It needs relatively much calculation power and high memory usage and can also be difficult to tune [3]. At each time step, the EKF makes a linearization around the current working point, if this linearization is a poor approximation, the EKF will converge poorly or worse even diverge [3].

Because of this, alternative observers were also considered.
The choice of observer to compare against the EKF observer was an Averaging Observer and can roughly be described as it takes the mean between the measurement and the prediction. This observer method is very simple, but as proven later, it delivers results good enough for this application, which raises the question about the trade off between the observer's complexity and its performance.

3.2 Extended Kalman Filter

The EKF is a stochastic observer and takes the sensor noise into account. It estimates the states such that the root mean square of the error is minimized.
The EKF process can be divided into two phases.

Predict

$$x_{k|k-1} = f(x_{k-1|k-1}, u_k)$$
$$P_{k|k-1} = F_k P_{k-1|k-1} F_k^T + W_k Q W_k^T$$

Update

$$y_k = z_k - h(x_{k|k-1})$$
$$S_k = H_k P_{k|k-1} H_k^T + V_k R V_k^T$$
$$K_k = P_{k|k-1} H_k^T S_k^{-1}$$
$$x_{k|k} = x_{k|k-1} + K_k y_k$$
$$P_{k|k} = (I - K_k H_k) P_{k|k-1}$$

Where F_k and H_k are the Jacobians of $f(x_{k-1|k-1}, u_k)$ and $h(x_{k|k-1})$ with respect of x, and W_k and V_k are the Jacobians of $f(x_{k-1|k-1}, u_k)$ and $h(x_{k|k-1})$ with respect of process noise and measurement noise.

$f(x_{k-1|k-1}, u_k)$ is the nonlinear vehicle model which predicts the states $x_{k|k-1}$ at time *k* based on the states $x_{k-1|k-1}$ from time *k-1* and external inputs u_k, example wheel steer angle.

$P_{k|k-1}$ is the predicted error covariance matrix at time *k*, based on the Jacobian of the vehicle model F_k, the predicted error covariance matrix $P_{k-1|k-1}$ from time *k-1* and the process noise covariance matrix Q.

y_k is the measurement residual at time k based on measurements z_k and predicted measurements $h(x_{k|k-1})$.

S_k is the residual covariance at time k based on the Jacobian of the predicted measurements function H_k, predicted error covariance matrix $P_{k|k-1}$ and measurement noise covariance matrix R.

K_k is the optimal Kalman gain at time k based on the Jacobian of the predicted measurements function H_k, predicted error covariance matrix $P_{k|k-1}$ and the residual covariance.

The states $x_{k|k}$ and predicted error covariance matrix $P_{k|k}$ at time k can then be calculated based on optimal Kalman gain K_k, measurement residual y_k, Jacobian of the predicted measurements function H_k and the predicted error covariance matrix $P_{k|k-1}$.

3.3 Averaging Observer

The main idea behind this observer is that the true state value most probably is somewhere between the predicted state value and the measured state value.
With possibility to weight the predicted and measured state differently, the estimated state value is calculated as an average of the two weighted states.
This method has several analogies with a P-controller with the weights corresponding to the P-controllers gain K.
Because of this, some theory used for the P-controller apply to this observer. Example if the weights which correspond to the gain K are chosen incorrect the observer might not converge.
The P-controller is known to under some conditions give steady state errors and never reach its target value. This is normally handled by use of a PI-controller which introduces an integration part.
In this observer there is no problem with steady state errors except sometimes on the longitudinal velocity estimation. Therefore the longitudinal velocity estimation is compensated with the sum of the past differences between predicted velocities and measured velocities, which corresponds to the integration part of a PI-controller.
Like the PI-controller the integral gain has to be chosen carefully to avoid instability.

$$x_t^{predicted} = f(x_{t-1}^{estimated}, u_t)$$

$$x_t^{estimated} = \frac{w_1 \cdot x_t^{predicted} + w_2 \cdot x_t^{measured}}{w_1 + w_2} + w_3 \sum_{s=0}^{t} \left(x_s^{measured} - x_s^{predicted} \right)$$

w_1, w_2 and w_3 is the observers tunable parameters.

w_1 is how much one rely on the model and w_2 is the measurement reliability which should be small if much measurement noise is expected.

w_3 is the gain of the integration part which serves to reduce steady state errors. On the analogy of the integration part of a PI-controller, this gain can also introduce instability. w_3 is preferably in this work kept to zero with exception for the longitudinal velocity.

It should be clarified that when this method is implemented the summation of $s = 0 \ldots t$ in the later equation does not have to be entirely recalculated each time step, it is only necessary to add the latest difference to the previous summation.

$$S_t = S_{t-1} + (x_s^{measured} - x_s^{predicted})$$

$$x_t^{estimated} = \frac{w_1 \cdot x_t^{predicted} + w_2 \cdot x_t^{measured}}{w_1 + w_2} + w_3 S_t$$

This observer biggest advantage is that it's compared to EKF is very light on computations and are also easier to tune correctly.

3.4 Road friction coefficient estimator

Knowledge about the road friction coefficient μ is very important to give good estimation on the lateral velocity because it affect the tire forces and thereby the vehicle handling dynamics. It can vary from about 0.1 on ice and about 1.0 on dry asphalt. Like the lateral velocity is there in commercial passenger cars by economical reasons not possible to measure the friction coefficient. Instead it has to be estimated.

While driving straight ahead with no longitudinal or lateral wheel slip it is impossible to estimate the road friction coefficient, because in this region the tire forces are not dependent of the road friction μ, se Figure 3.2.

If driving straight ahead with wrong estimated μ and quickly turning the steering wheel, the model may fail to predict the vehicle behavior, because the friction estimator have too little time to adjust the value of μ.

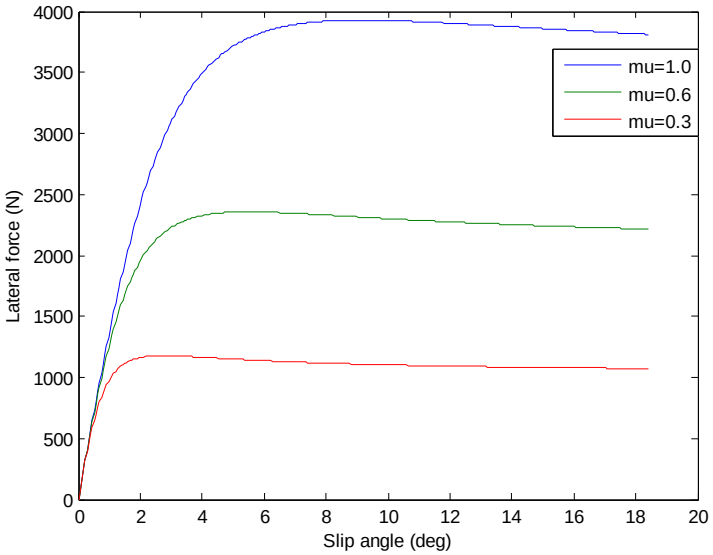

Figure 3.2 – Tire lateral force at different μ. (Magic Formula)

Estimation based on lateral acceleration
One possibility is to compare the estimated lateral acceleration with the measured acceleration. If the estimated acceleration is lesser than the measured one can conclude that the used friction coefficient is probably to low.
This method relies on a good lateral acceleration measurement, but as shown later in this report, a good lateral acceleration measurement can be hard to get.

$$\mu_{new} = \mu_{old} + K \cdot \left(a_y^{estimated} - a_y^{measured}\right) \cdot sign\left(v_y^{estimated}\right)$$

The choice of the gain *K* is a trade off between stability and speed of convergence.

Estimation based on longitudinal slip
There is also possible to estimate the friction by use information about the driveline torque, the wheel angular velocities and the vehicle velocity.
The wheel angular velocities and the vehicle velocity gives a measurement of the tires longitudinal slip and by comparing the slip with the applied torque the friction coefficient can be estimated.
If example wheel spin is detected at use of a relatively low driveline torque the friction can be estimated to be low.
This method tends to give a noisy and unstable estimation of the friction coefficient and need quite large longitudinal slip to give a good estimation.

Estimation based on yaw-rate
By comparing the estimated yaw-rate change with the measured yaw-rate change, information about the road friction coefficient can be estimated.
The yaw-rate change is a function of the tire forces because it is primarily the momentum created by the tire forces which produces the yaw-rate change.

$$\ddot{\psi}^{estimated} = \sum_{i=1..4} \frac{M_{Tire}^{i}}{I_{zz}} =$$

$$\frac{1}{I_{zz}}((F_{FLx} + F_{FRx})\, L_F \sin(\delta) + (F_{FLy} + F_{FRy})\, L_F \cos(\delta) - (F_{RLy} + F_{RRy})\, L_R +$$

$$(-F_{FRy} \sin(\delta) + F_{FRx} \cos(\delta) + F_{RRx})\, d_R + (F_{FLy} \sin(\delta) - F_{FLx} \cos(\delta) - F_{RLx})\, d_L)$$

Whether this approach is possible to use is not covered in this work. Brief tests have shown that this method sometimes estimates the friction coefficient accurate but it is most likely to have quite narrow convergence region and should only work as a complement to an already existing friction estimator.

4. Evaluation

4.1 Overview

In this section the different observers are tested and evaluated. This by comparing from the observers estimated states with reality. To represent reality a simulation from a more accurate and advance vehicle model can be used or if available, use experimental data from real world measurements.

In this work both simulation and experimental data have been used for observer evaluation.
The simulation model is a two track model, made in MATLAB Simulink and the experimental data is from Haldex AB proving ground in Arjeplog.

The in the plot presented "Rear axle slip angle" is simply the angle between the longitudinal velocity vector and the lateral velocity vector at the rear axle.

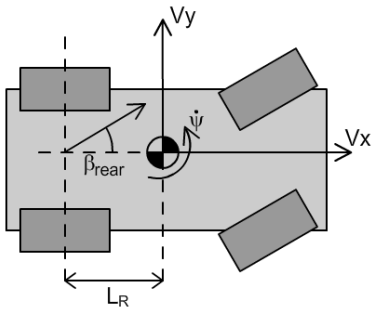

Figure 4.1 – Rear axle slip angle

$$\beta_{rear} = \tan^{-1}\left(\frac{v_y - L_R\dot{\psi}}{v_x}\right)$$

It is preferred to plot the slip angle instead of the lateral velocity because the slip angle takes the longitudinal velocity into account. Moreover, the slip angle plotted in the graphs below has been transposed to the rear axle, this is to get a measure emphasized on over steer situations, doing so we also don't have to deal with negative attitude angles at low vehicle speed.

4.2 MATLAB-Simulink

In this section the observer is evaluated against a six degrees of freedom Simulink model.
The Simulink model uses a more complex version of Magic Formula tire that models e.g. combined slip, lateral stiffness, cornering stiffness and relaxation length.

The measurement given to the observer is:

- Longitudinal velocity
- Lateral acceleration
- Yaw-rate

These measurement signals are plotted separately at the top of every test page. The estimated values of these states are not plotted in this report, because in all tests are the measurement and estimation in the plot almost inseparable and therefore not providing any extra information.
The data in the plot labeled "measurements" are the states of the Simulink model with added noise.

In the case of the measured change of lateral velocity ($v_y\ dot$) is:

$$\dot{v}_y^{measured} = a_y^{measured} - v_x^{estimated}\dot{\psi}^{estimated}$$

It is also possible to instead use:

$$\dot{v}_y^{measured} = a_y^{measured} - v_x^{measured}\dot{\psi}^{measured}$$

The first method is used because tests have shown that it gives better results.

Even if the sensor signal $a_y^{measured}$ does not look overwhelming noisy, it appears that $\dot{v}_y^{measured}$ have very more noise, this because the subtracted term $v_x^{estimated}\dot{\psi}^{estimated}$ is such a large part of the $a_y^{measured}$.

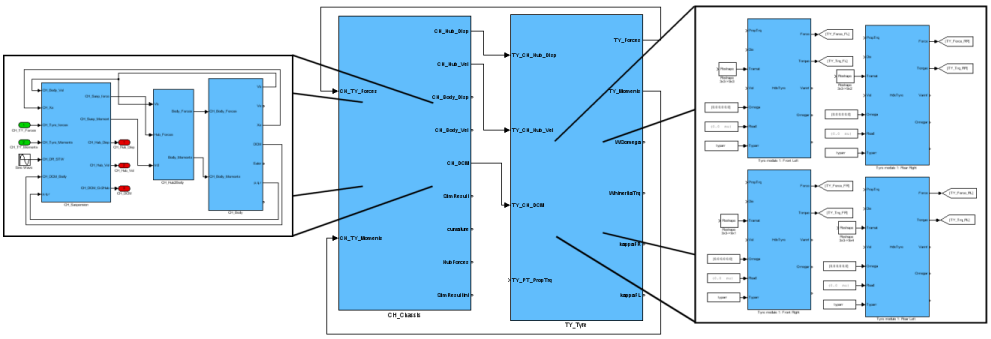

Figure 4.2 – A Simulink model

In all tests with a sinus sweep maneuver the initial steer angle direction is to left and in case of steer ramp maneuver the steer angle direction is also left.

Test 1.1: Sinus sweep, $\mu = 1$

In this test the Simulink model is released at 20 m/s and turns the steering wheel like a sinus wave. The road friction constant μ is 1. There is no torque applied.

Both observers have at this test more difficulty to estimate the slip angle accurate at the end, but both observers deliver almost identical results.

It is possibly that this estimation offset is a result of that the maneuver hit an area where the tire model is less accurate.

Test 1.2: Sinus sweep, $\mu = 0.3$

The road friction constant μ is 0.3. No torque applied.

The Averaging Observer and EKF estimates the slip angle very much the same.
In this maneuver the vehicle balances between the linear and non-linear tire characteristics. At time 12s the observer incorrect tips over into the non-linear area which immediately results in a less accurate estimation.

Test 1.3: Sinus sweep at high speed, $\mu = 0.7$

This test is performed with an initial longitudinal velocity of 50 m/s.

In this test the EKF performs slightly better. One reason is because the EKF more strictly follow the lateral acceleration sensor and therefore are able to reduce errors faster, provided that the signal from the sensor is correct.

Test 1.4: Sinus sweep, $\mu = 1$, slide

Also in this test it is hard to distinguish the both observers which perform much the same. The estimation is very accurate until time 8s, despite the big slip angle. After time 8s is the longitudinal velocity very low.

Test 1.5: Steer ramp, $\mu = 1$

In this test the steering wheel gets a ramp signal beginning at 0 at time 2s.

The estimation error in this test is relatively small for both observers. In the later part of the test the EKF estimation gets a bit nervous, maybe it is tuned to rely a bit too much on the noisy acceleration sensor.

Test 1.6: Steer ramp, $\mu = 0.7$, torque applied

In this test the performance of the modeled combined slip is tested.
At time 7s the engine torque is increased rapidly to provoke wheel spin, the torque distribution is 70% at the rear axle.
The front and rear inside wheel spin most because of the load transfer to the outside wheels.

The combined slip model seems to reduce the available lateral grip quite well.

Test 1.1: Sinus sweep, $\mu = 1$

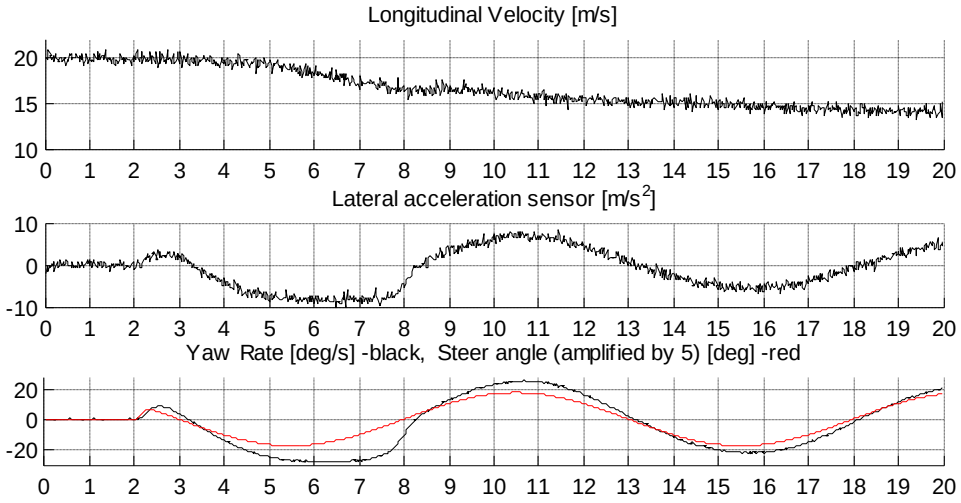

Extended Kalman Filter

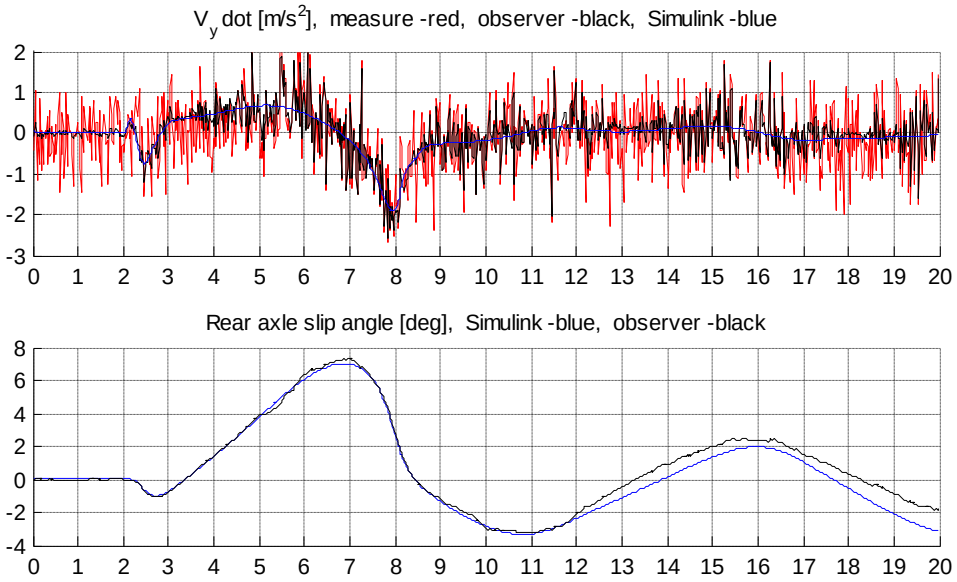

Averaging Observer

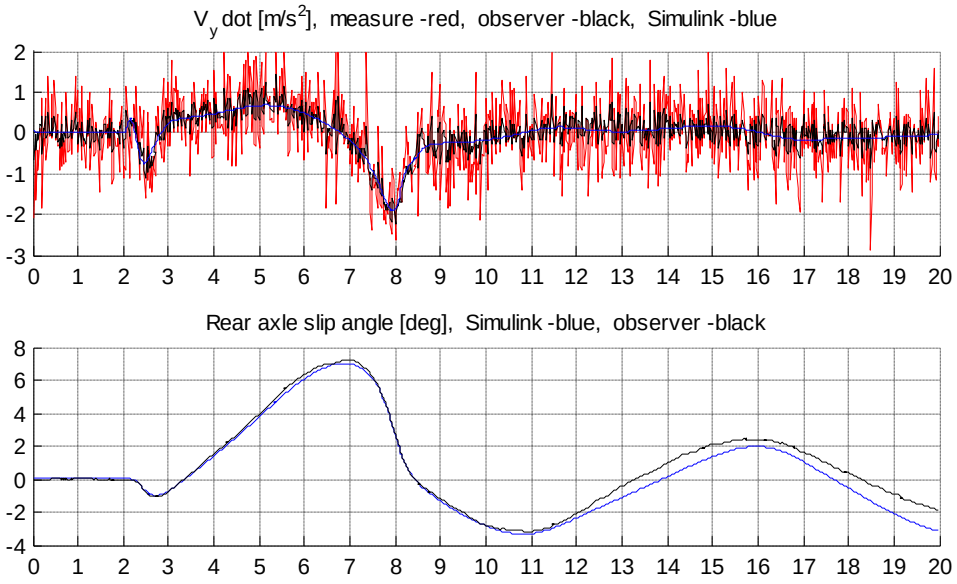

Test 1.2: Sinus sweep, $\mu = 0.3$

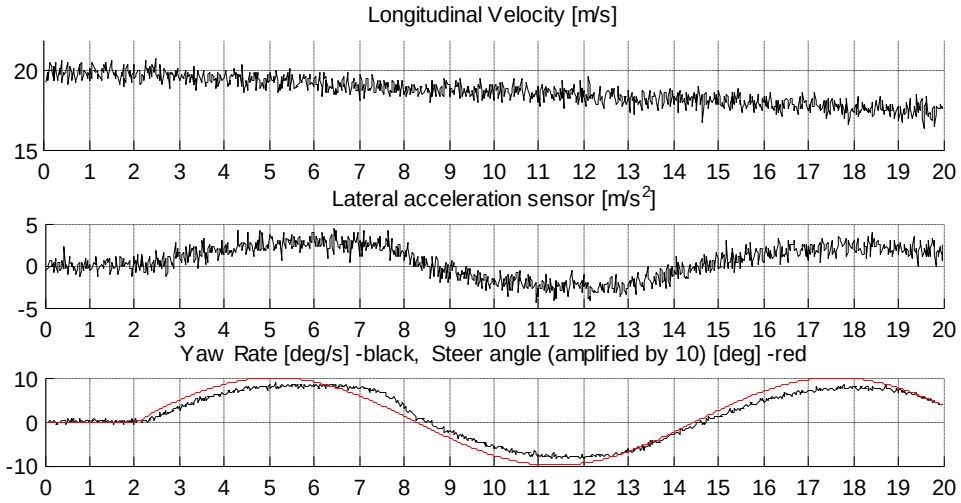

Extended Kalman Filter

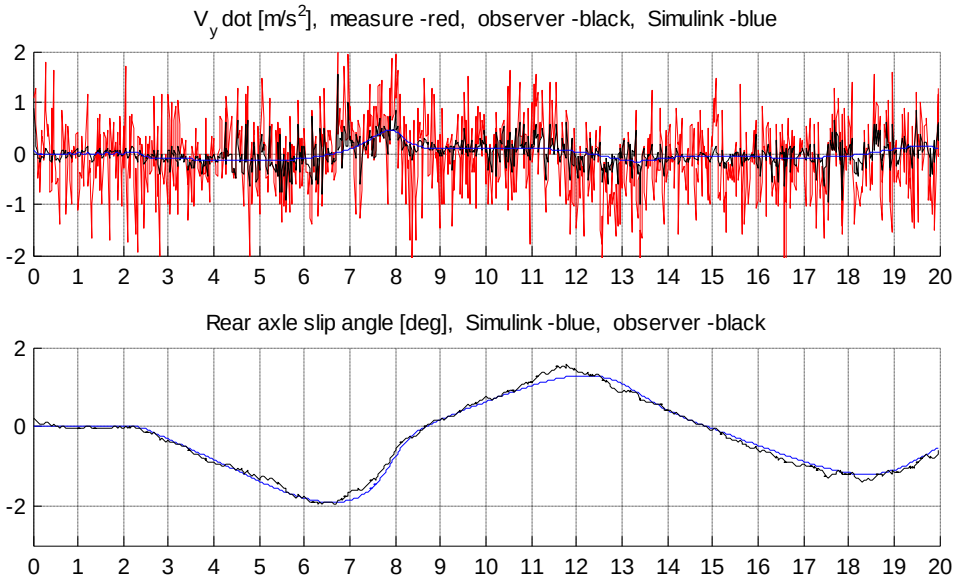

Averaging Observer

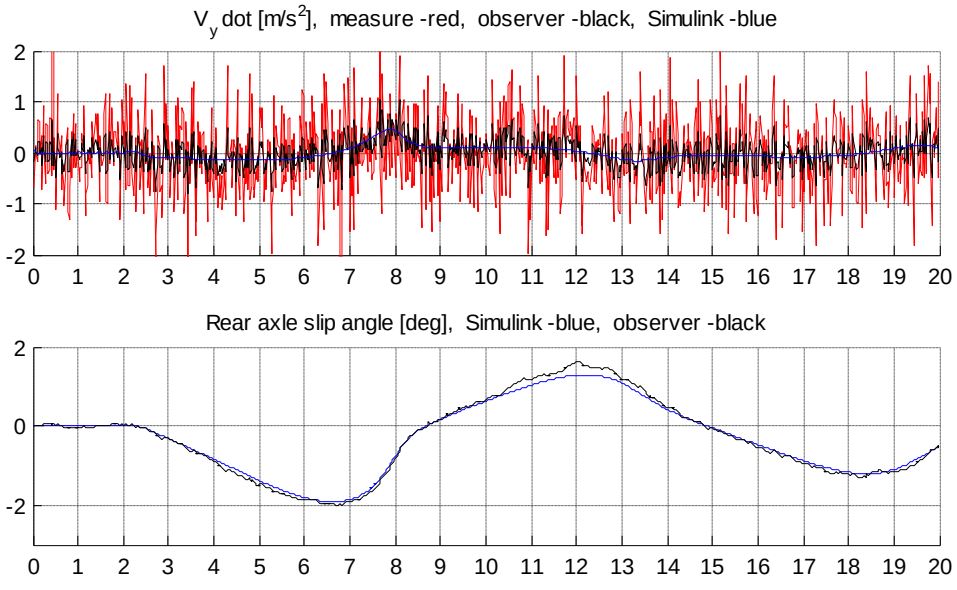

Test 1.3: Sinus sweep at high speed, $\mu = 0.7$

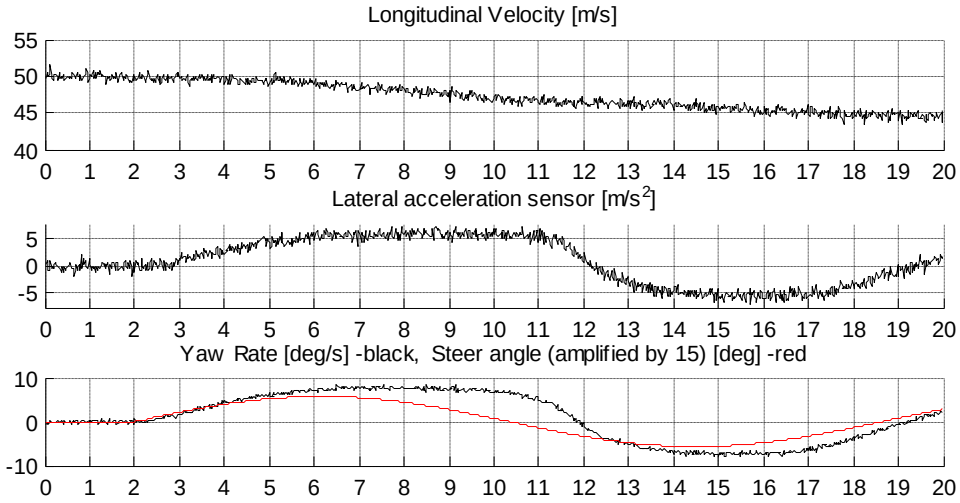

Extended Kalman Filter

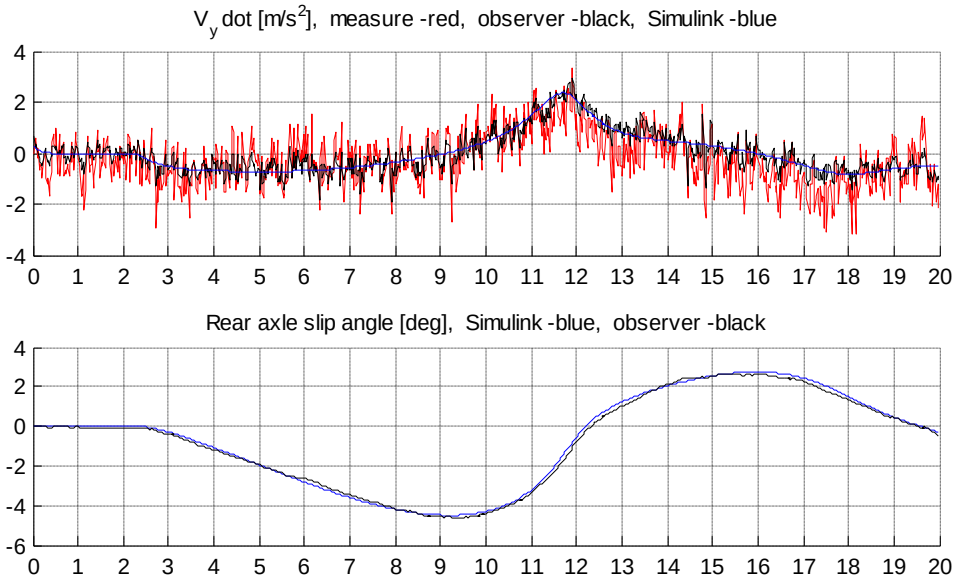

Averaging Observer

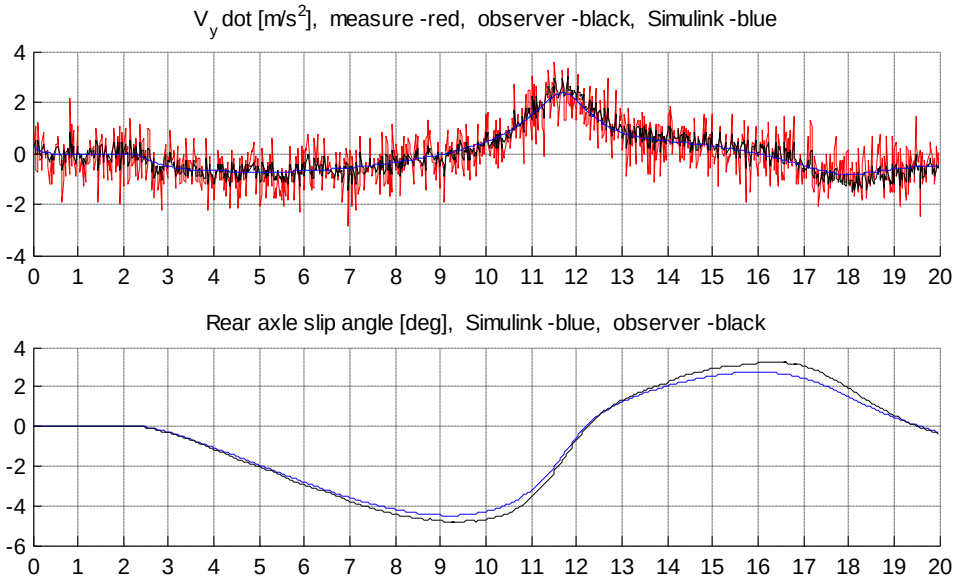

Test 1.4: Sinus sweep, $\mu = 1$, slide

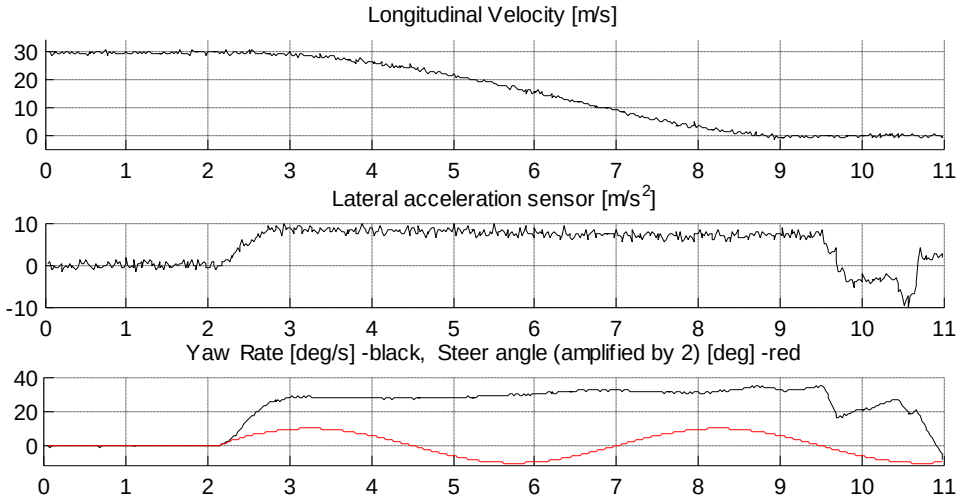

Extended Kalman Filter

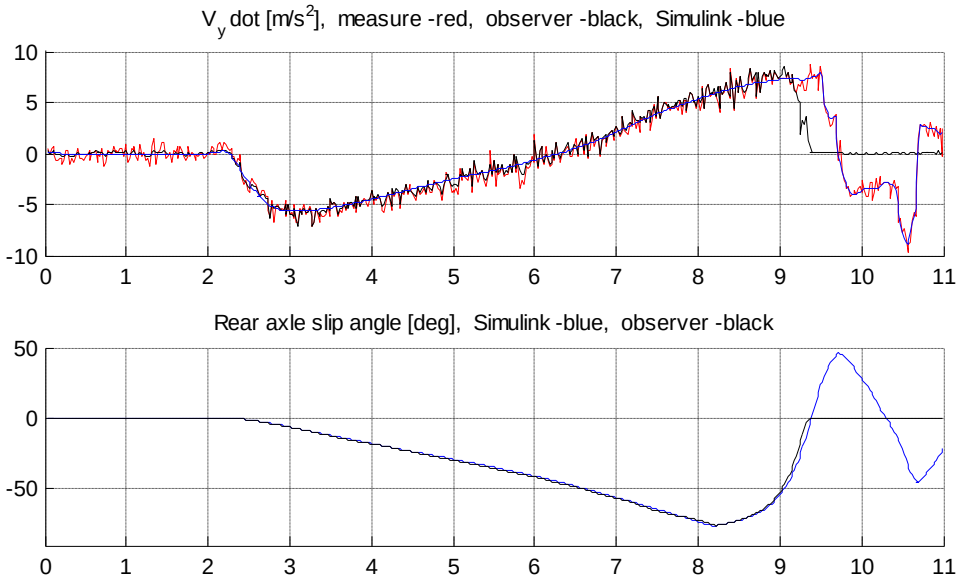

Averaging Observer

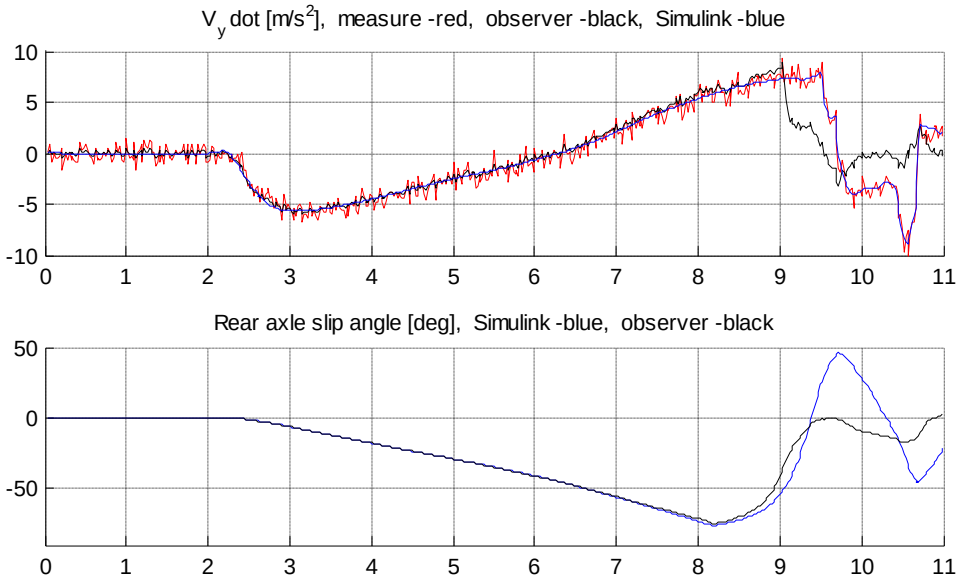

Test 1.5: Steer ramp, $\mu = 1$

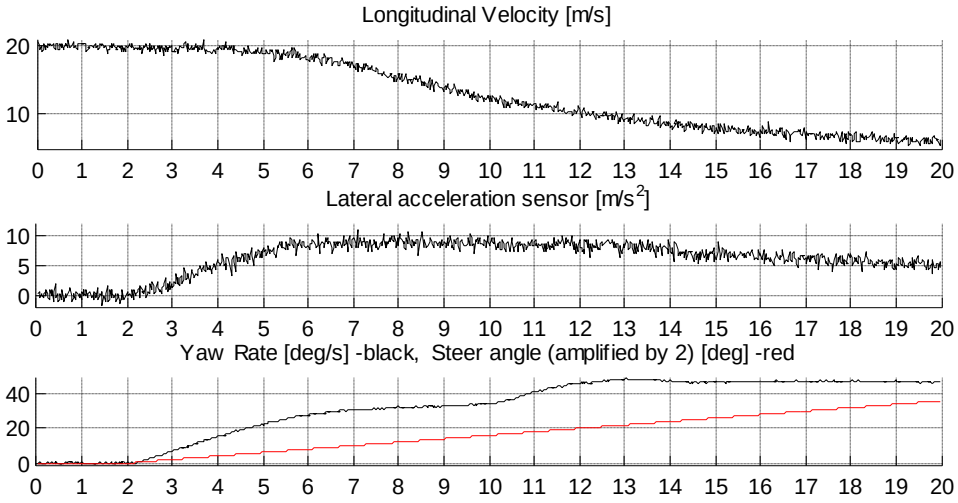

Extended Kalman Filter

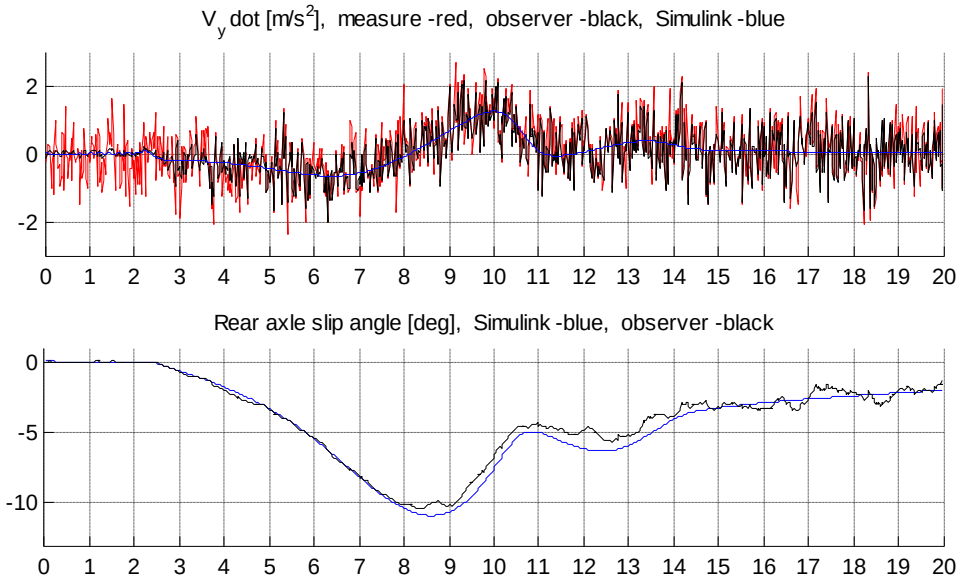

Averaging Observer

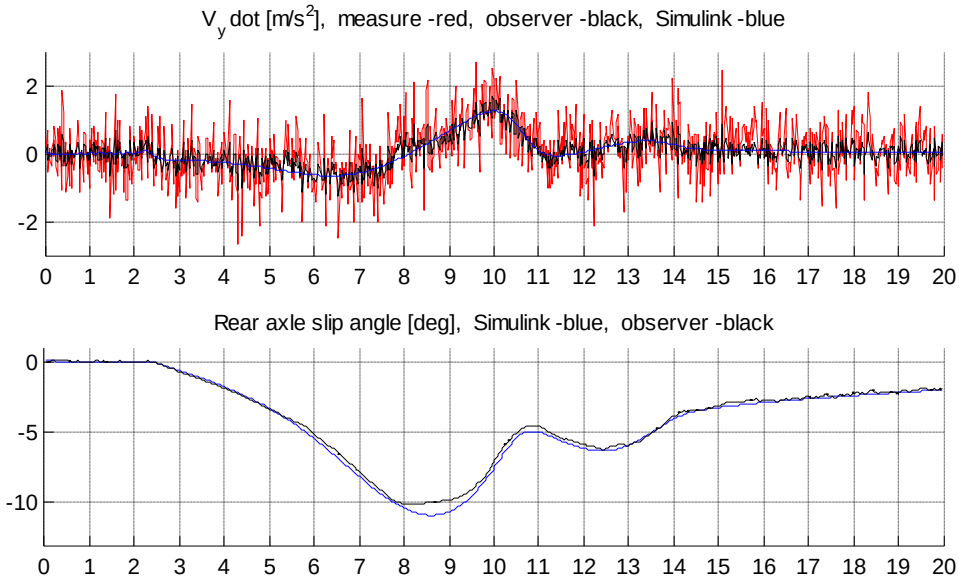

Test 1.6: Steer ramp, $\mu = 0.7$, torque applied (70% on rear axle)

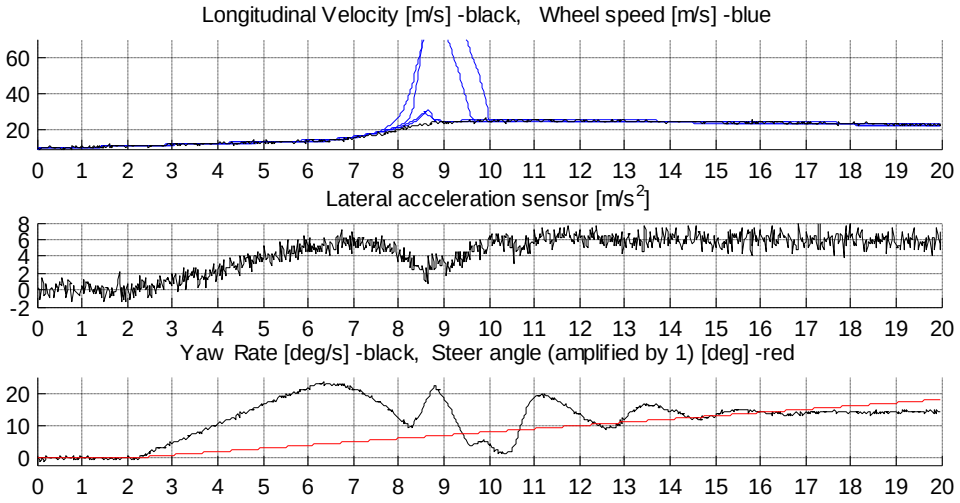

Extended Kalman Filter

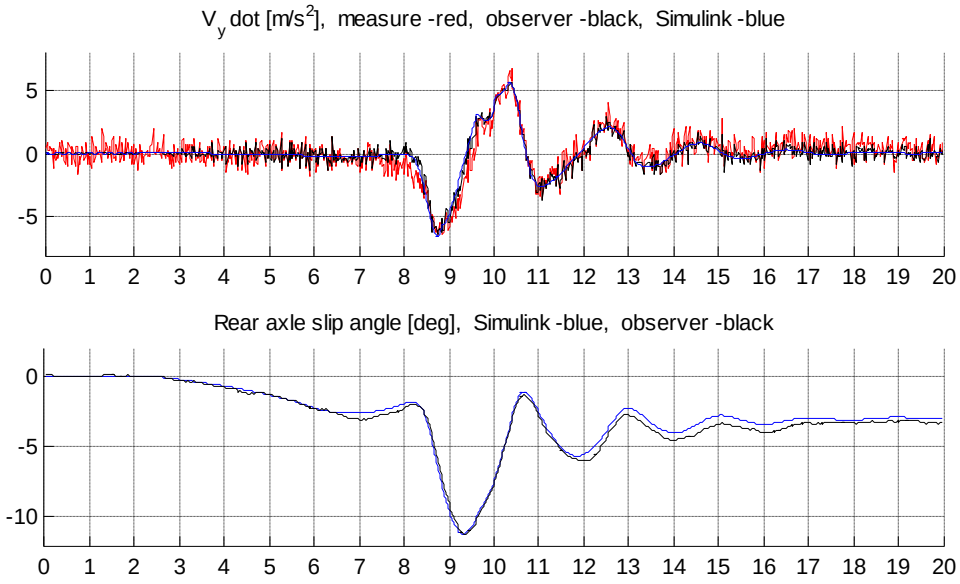

Averaging Observer

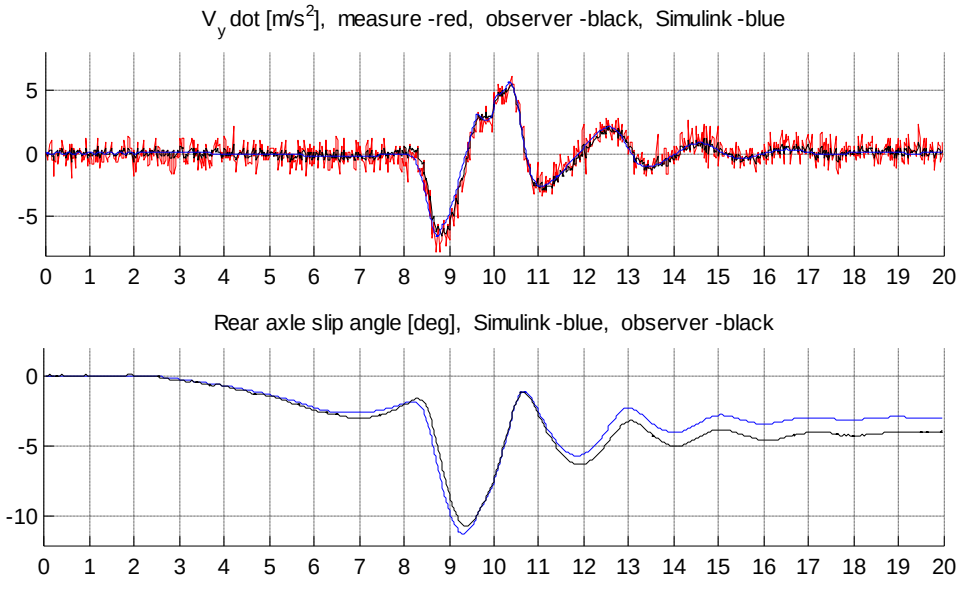

4.3 Experimental

The test vehicle used is a Volkswagen Bora V6 equipped with ESP and the Haldex Limited Slip Coupling. In addition this test vehicle is equipped with an optical sensor, which measures the longitudinal and lateral velocity over ground.

Figure 4.3 – Test vehicle equipped with an optical sensor

Because the optical sensor not is mounted in the center of the car but in front, the measured velocity has to be compensated for this to give the velocity at the center of the car.

In difference from the simulation environment the sensors have some amount of unknown offsets and scaling. The amount of disturbance of the lateral acceleration sensor is sometimes that big causing the observer to perform better without it. Therefore the tests have been done with both the lateral acceleration sensor active and inactive.

In these tests, same tire model was used as in the Simulink tests.
Each test was done at two cases:

1. Only the friction coefficient was allowed to be changed (black)
2. Friction coefficient and tire stiffness factor was allowed to be changed (blue)

At case 2 was the tire stiffness modified the same amount on all tests.

The tests are chosen to be hard for the observer to estimate accurate and take place into the tires non linear area most of the time.

The measurement given to the observer is:

- Longitudinal velocity
- Lateral acceleration (tests are done both with and without this sensor)
- Yaw-rate

Test 2.1: Steer step maneuver, $\mu = 0.35$.

In this test the results was more accurate when the observer didn't use the lateral acceleration signal. From time 9-11s the estimated value of $\dot{v}_y$ is too high because the lateral velocity isn't dropping as fast as it should. At the same time the lateral acceleration sensor delivers even higher values which are in the complete wrong direction.
In the case when the tire stiffness factor was changed the observer responded more correct on the steer input.
Both observers performed very much the same.

Test 2.2: Sinus sweep maneuver, $\mu = 0.35$.

At this test the estimated and the measured lateral velocity seems to have much the same amplitude but an increasing offset.
In Test 2.2a is the difference between the measured and the estimated $\dot{v}_y$ very different. Still are the measured and estimated lateral velocities relatively accurate. Therefore it is no surprise that in Test 2.2b when the observer tries to follow the measured $\dot{v}_y$, accuracy is lost.
At these tests the change of the tire stiffness factor didn't improve the result significant.

Test 2.3: Steer step maneuver, $\mu = 0.35$.

The large slip angle in this test indicates that vehicle is almost at the limit to a full spin out. The adjustment of the tire stiffness factor made it easier for the observer to stay on the correct solution.

Test 2.1a: Steer step maneuver, $\mu = 0.35$, lat.acc. sensor not used.

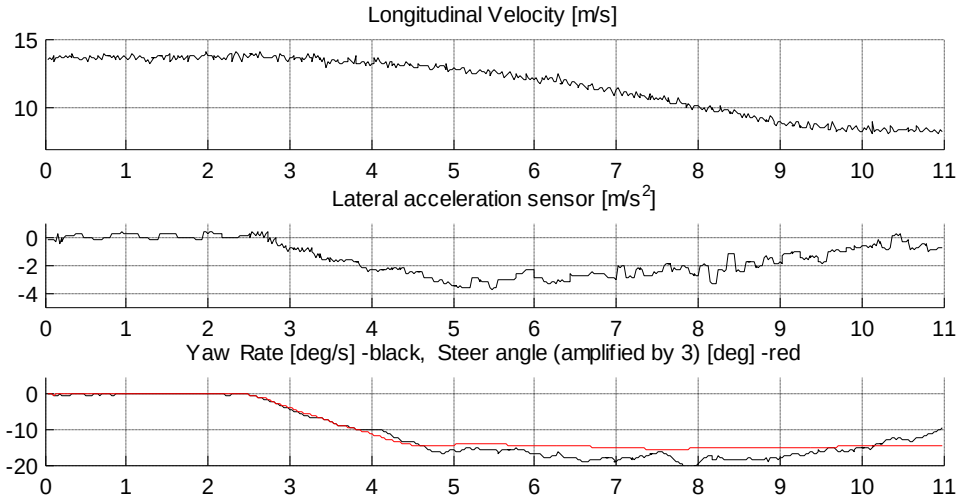

Extended Kalman Filter

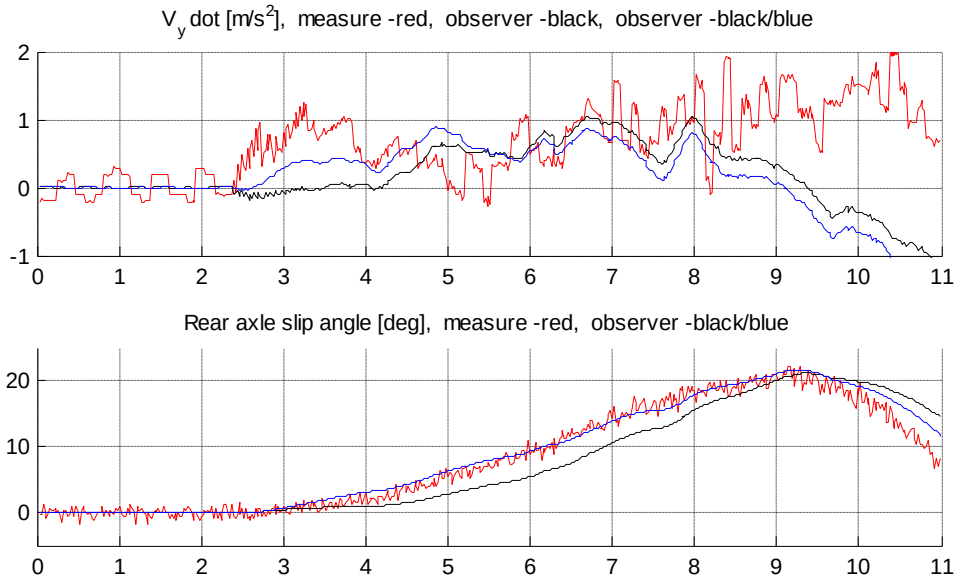

Averaging Observer

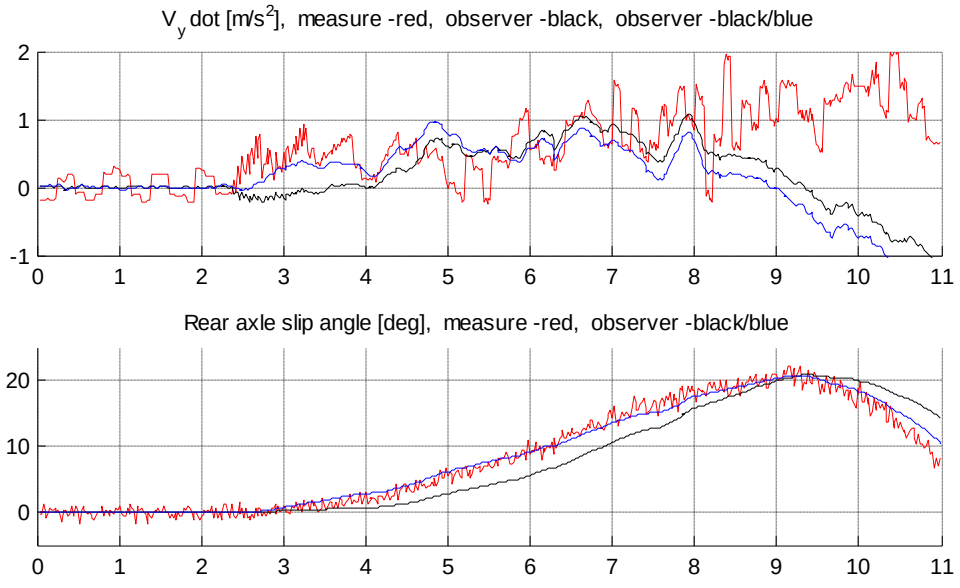

Test 2.1b: Steer step maneuver, $\mu = 0.35$, lat.acc. sensor used.

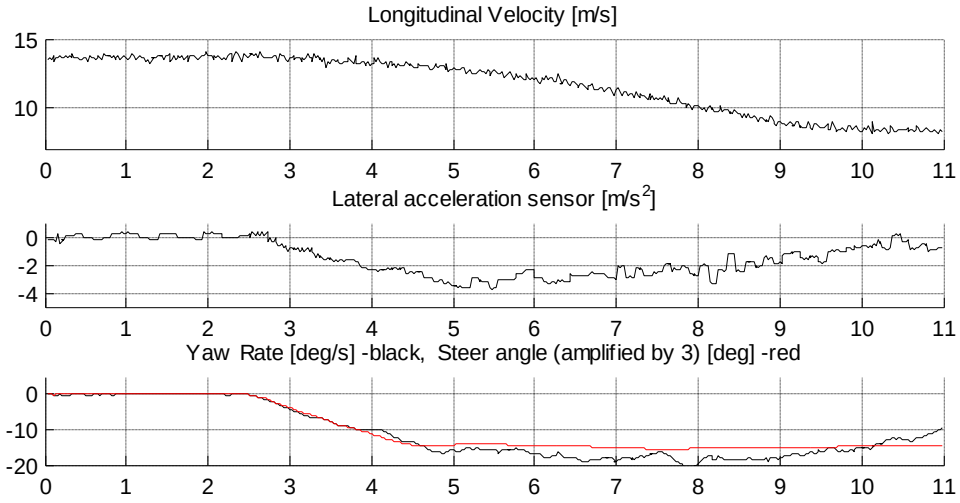

Extended Kalman Filter

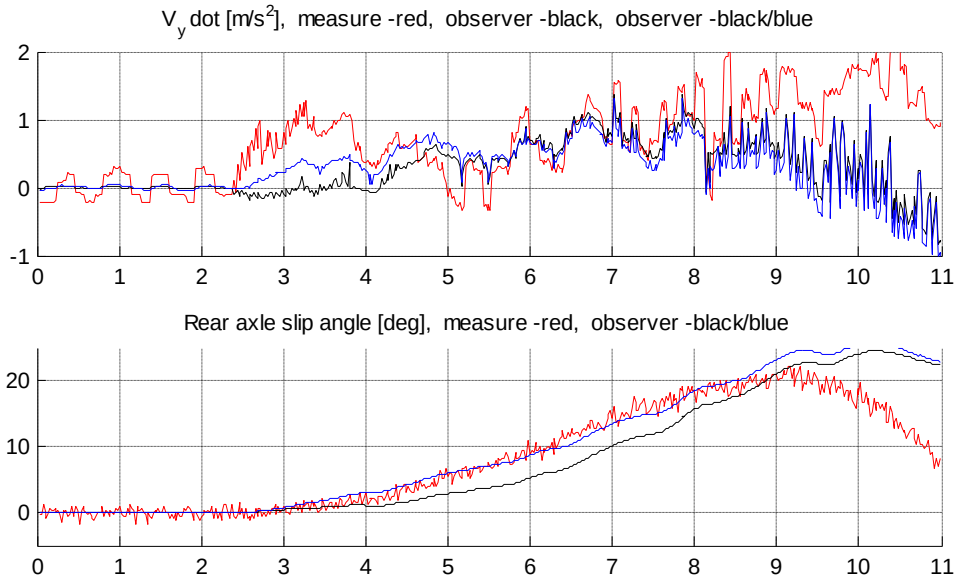

Averaging Observer

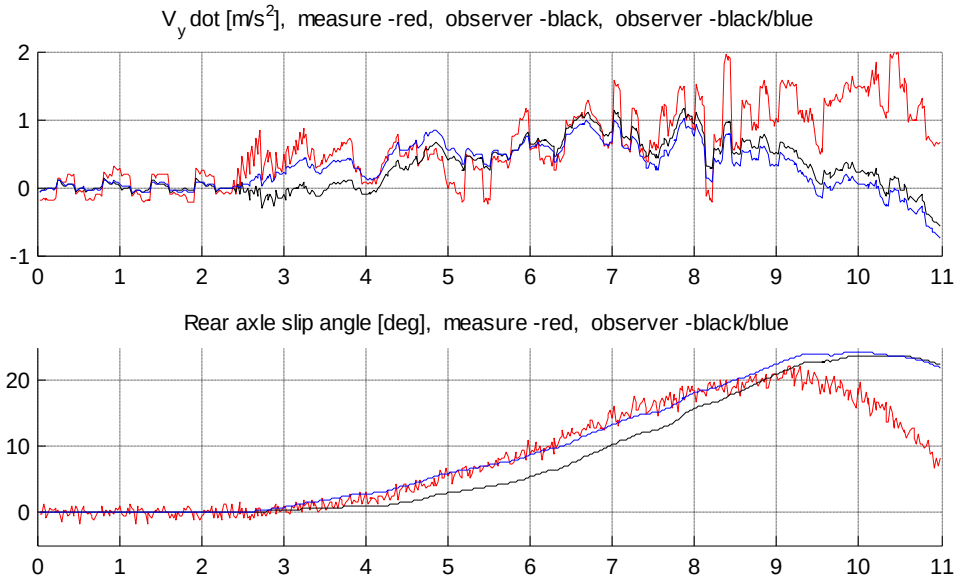

Test 2.2a: Sinus sweep maneuver, $\mu = 0.35$, lat.acc. sensor not used.

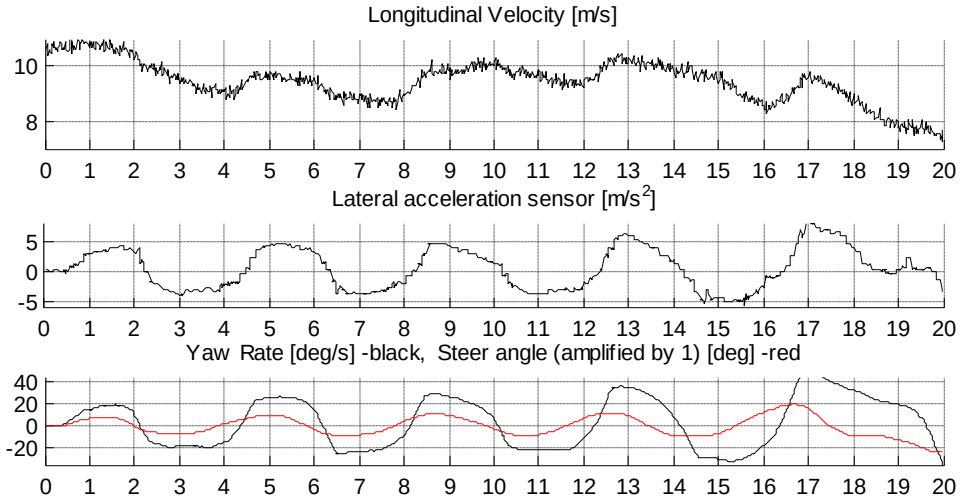

Extended Kalman Filter

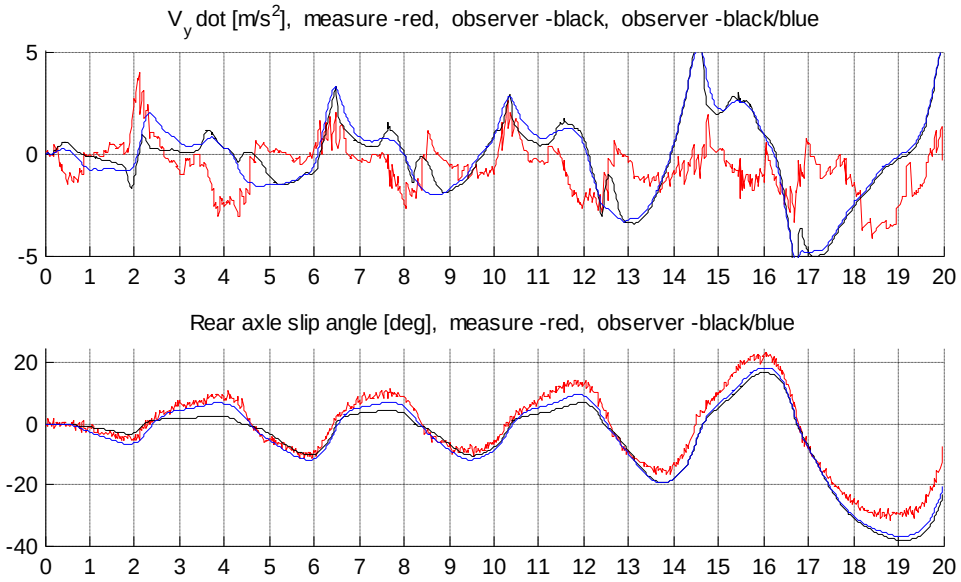

Averaging Observer

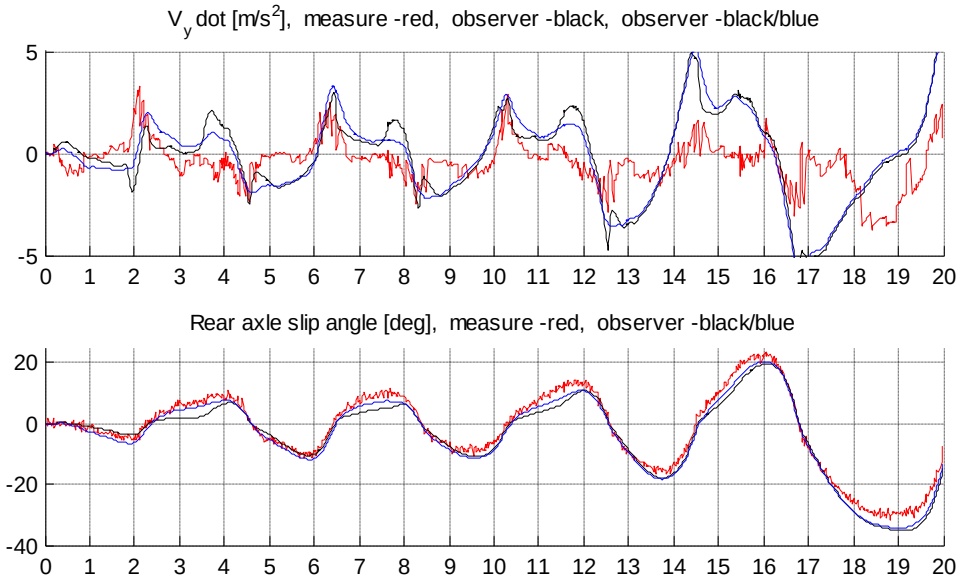

Test 2.2b: Sinus sweep maneuver, $\mu = 0.35$, lat.acc. sensor used.

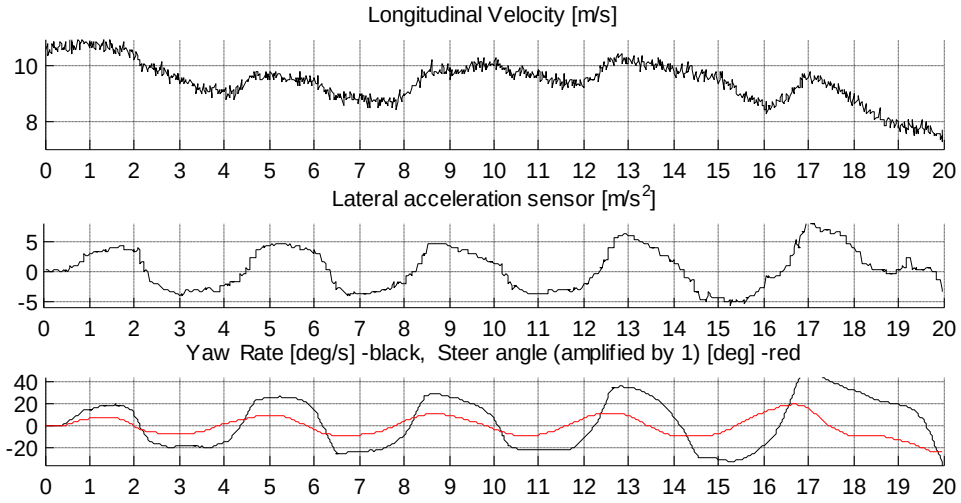

Extended Kalman Filter

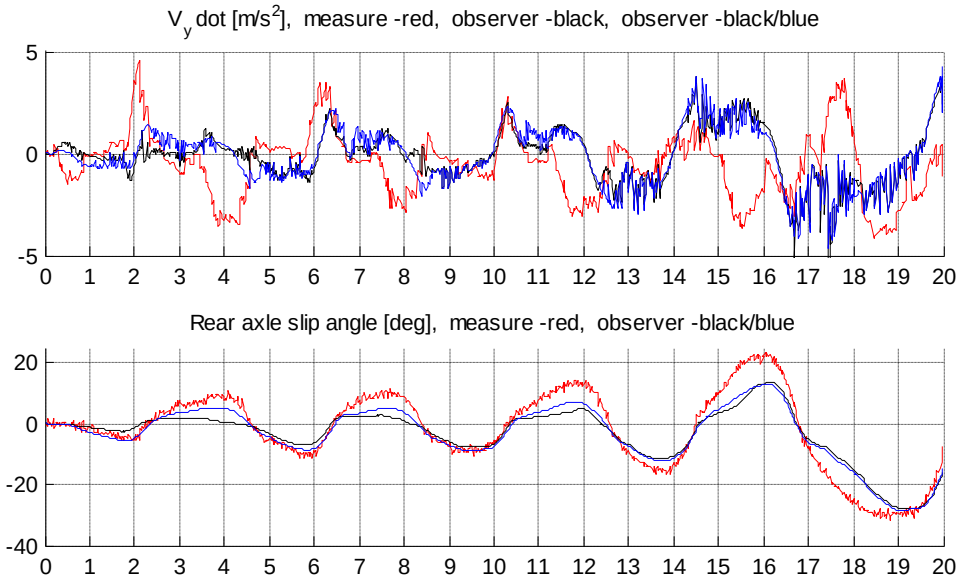

Averaging Observer

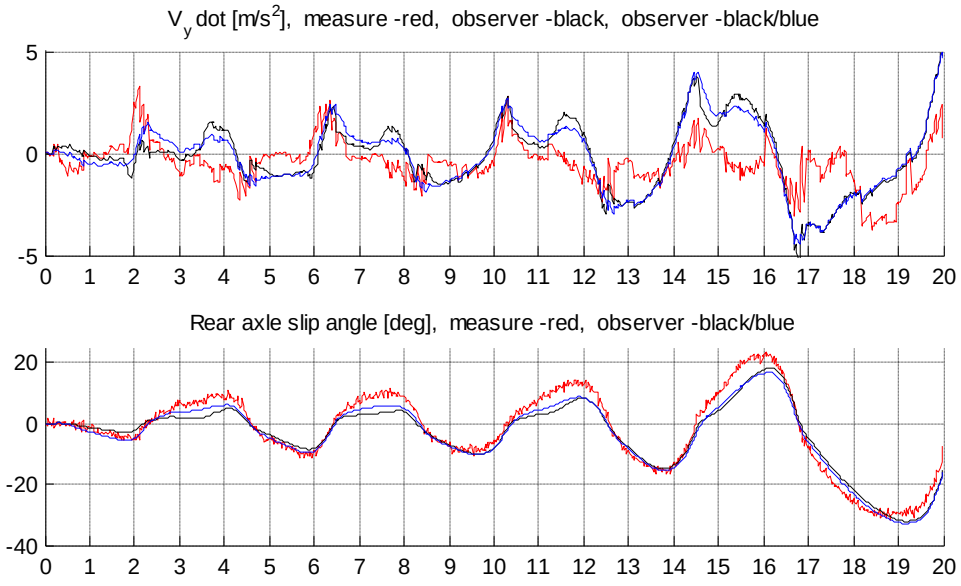

Test 2.3a: Steer step maneuver, $\mu = 0.35$, lat.acc. sensor not used.

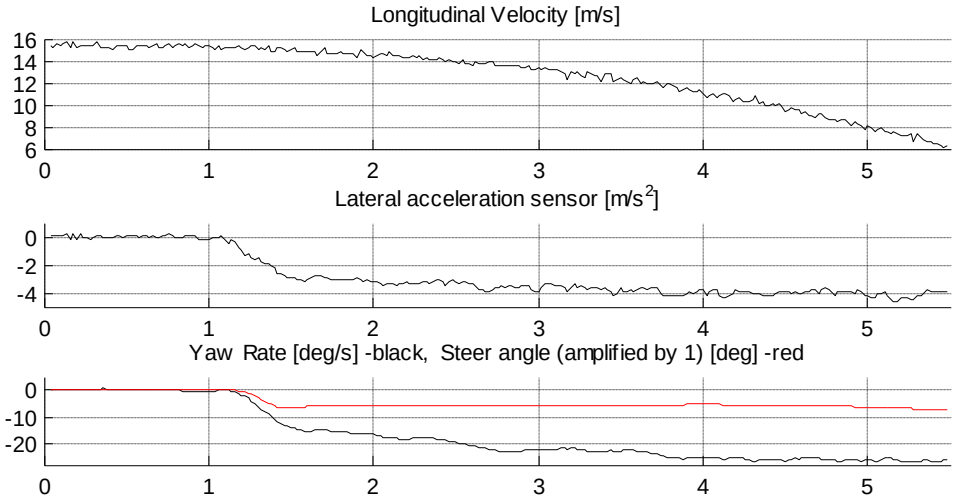

Extended Kalman Filter

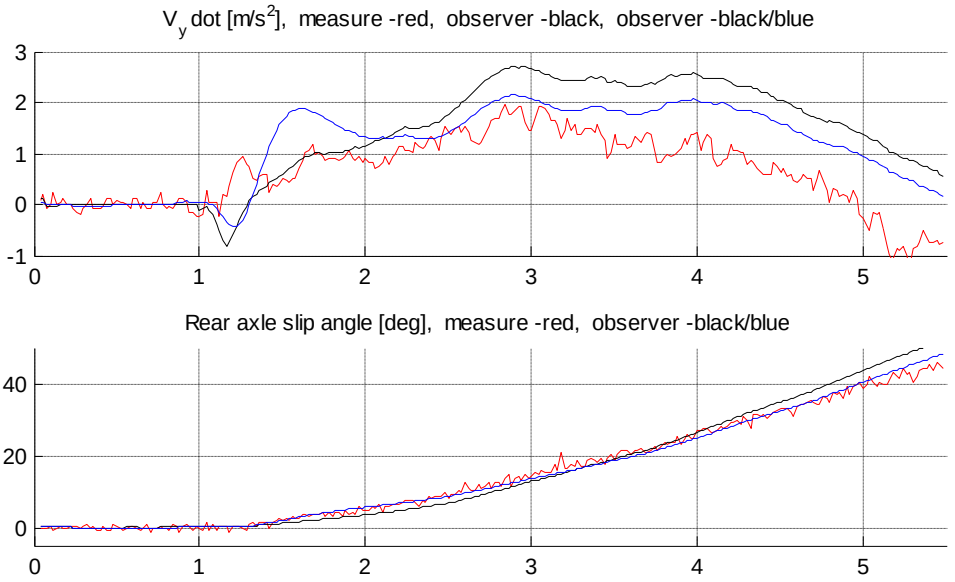

Averaging Observer

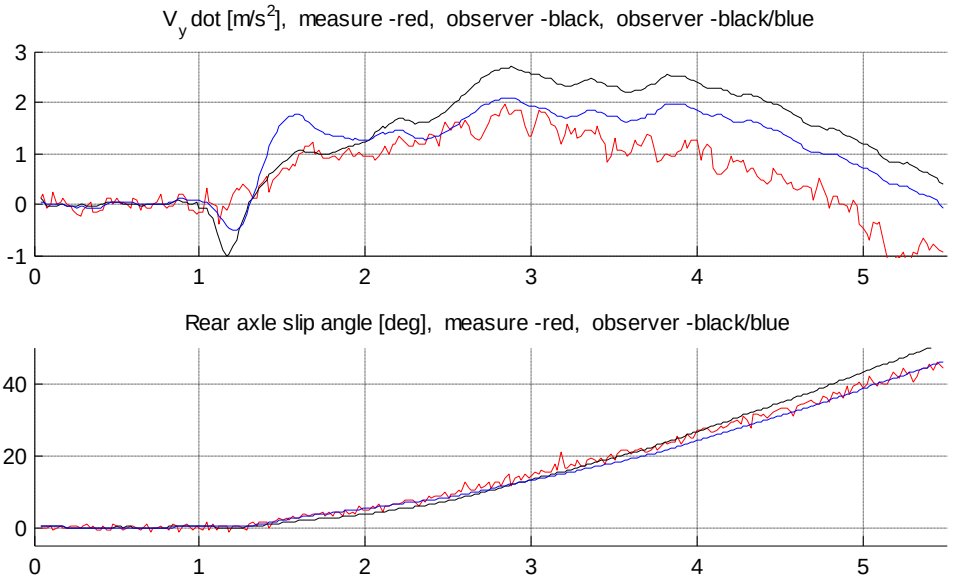

Test 2.3b: Steer step maneuver, $\mu = 0.35$, lat.acc. sensor used.

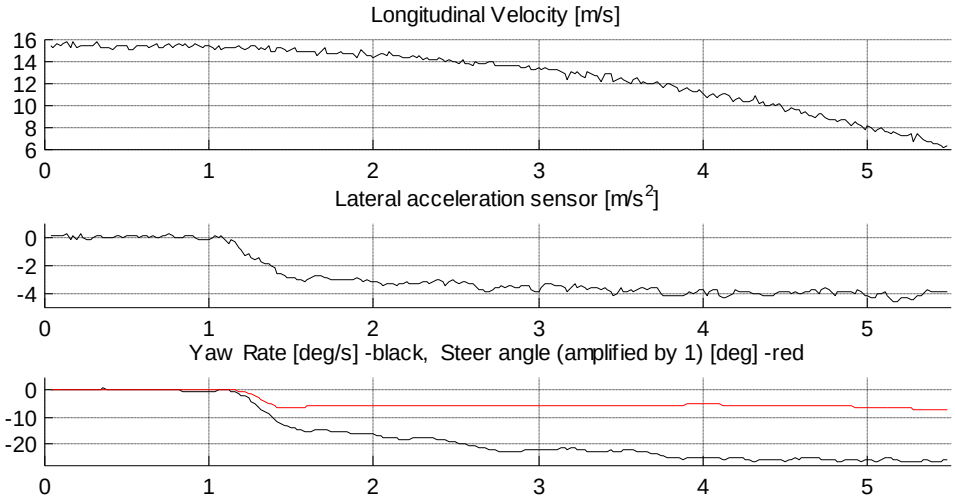

Extended Kalman Filter

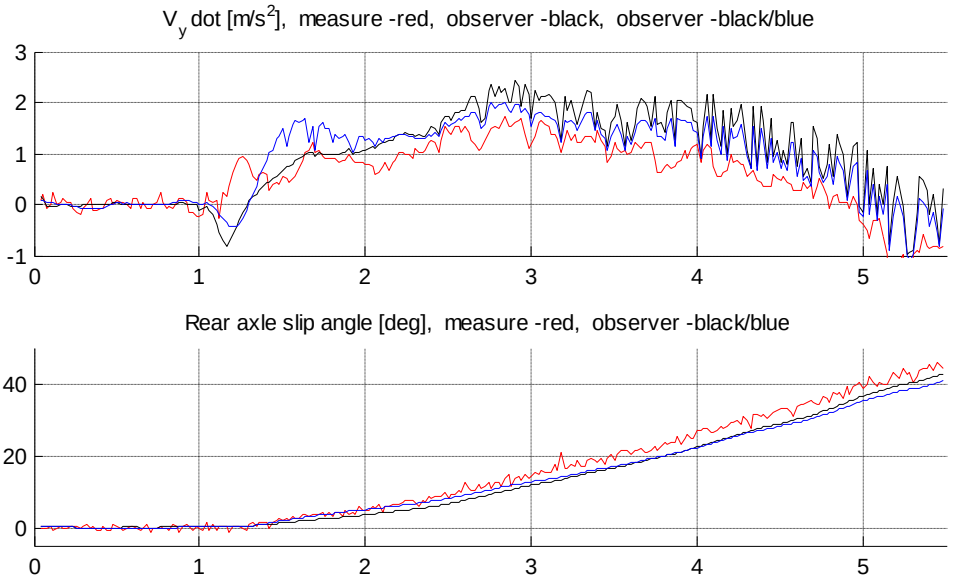

Averaging Observer

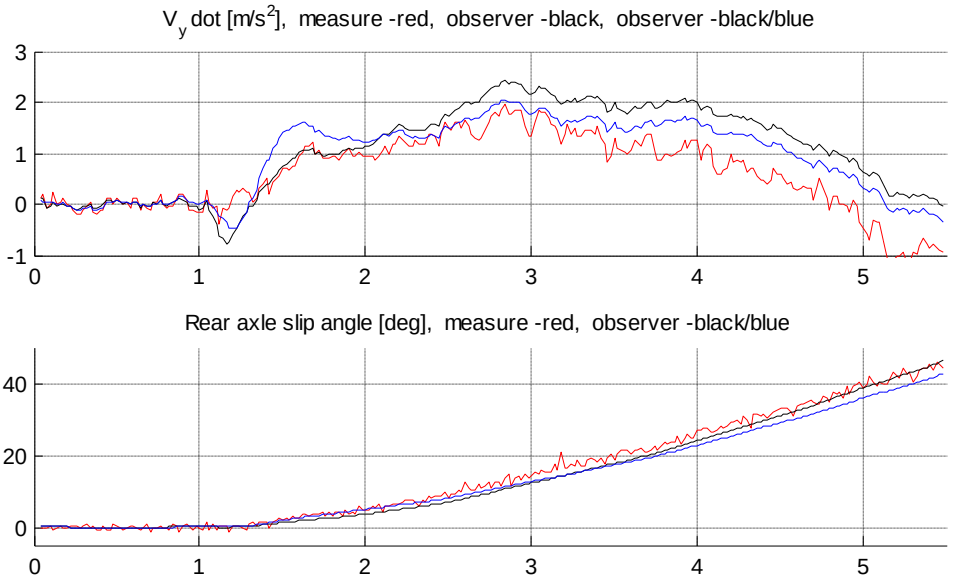

4.4 Road friction estimation

Test 3.1 - Simulink

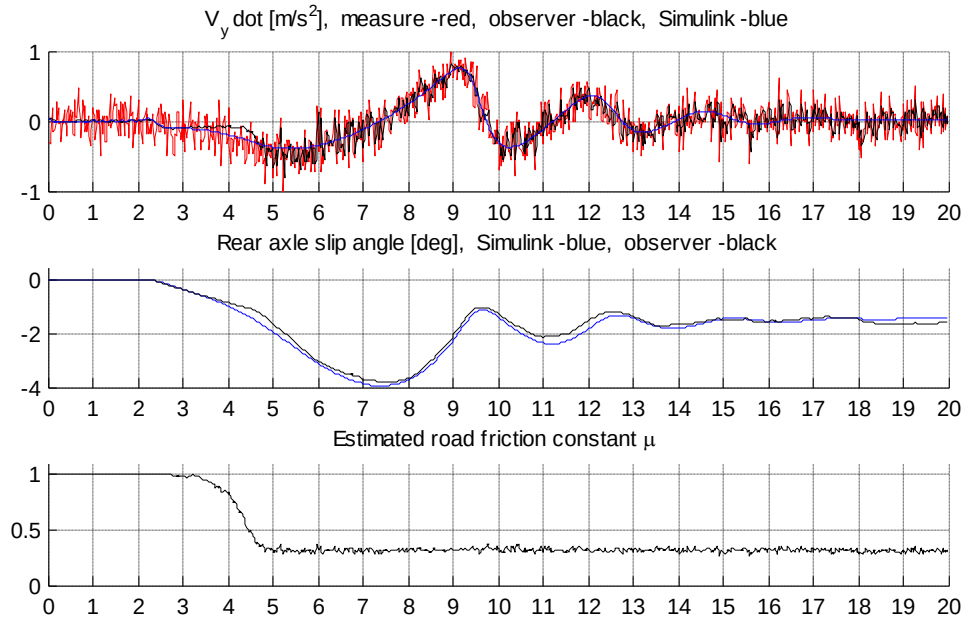

This is the same maneuver as in Test 1.6.
The road friction coefficient is on forehand set to 1 and are then estimated and adjusted by the observer. The estimation technique is explained in chapter 3.4 and the method in this test uses the lateral acceleration sensor.
The accurate and fast estimation is possible because the noise characteristics from the Simulink measurements are known well.

Test 3.2 - Simulink

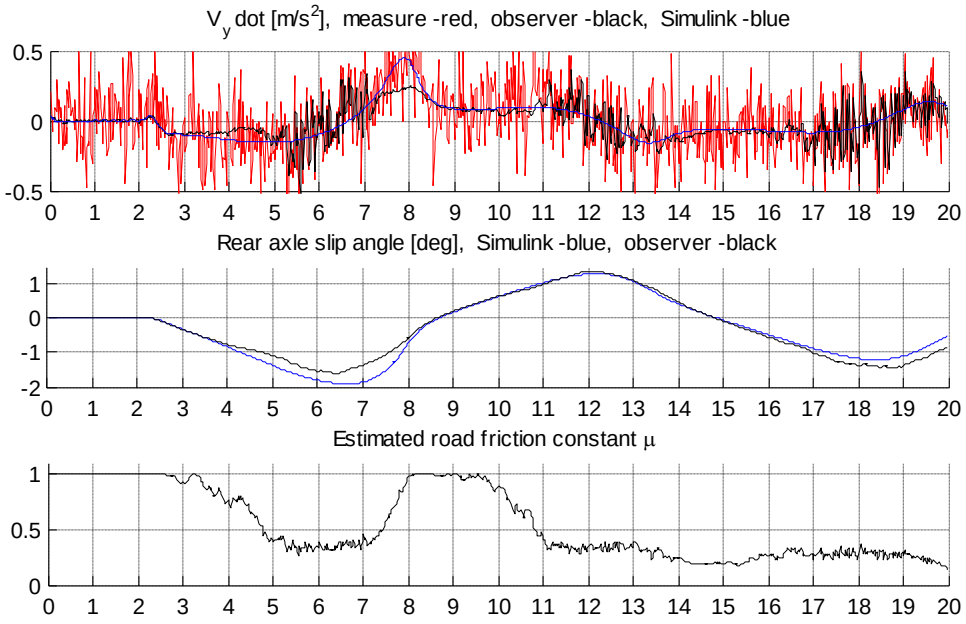

This is the same maneuver as in Test 1.2.
At the beginning the friction constant is set to 1, the observer realize at time 3s that μ has to be lowered but the estimation error of the slip angle caused by the high initial value of the friction coefficient mislead the friction estimator such that it at time 7s believes that the friction is set too low. Later the estimation find right track and start to converge.

Test 3.3 - Experimental

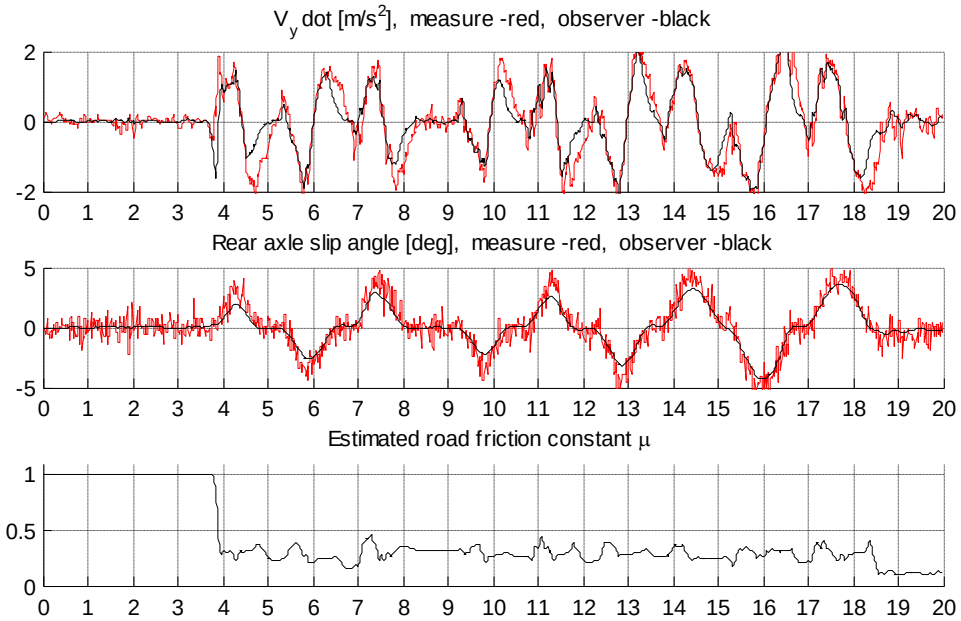

In this test the friction estimation works quite well. It converges but at a slightly too high value of the friction constant. The slope from time 4s and forward is overall downhill which is correct, but at several points the acceleration sensor incorrect tells the observer to momentarily increase the friction constant.

Test 3.4 - Experimental

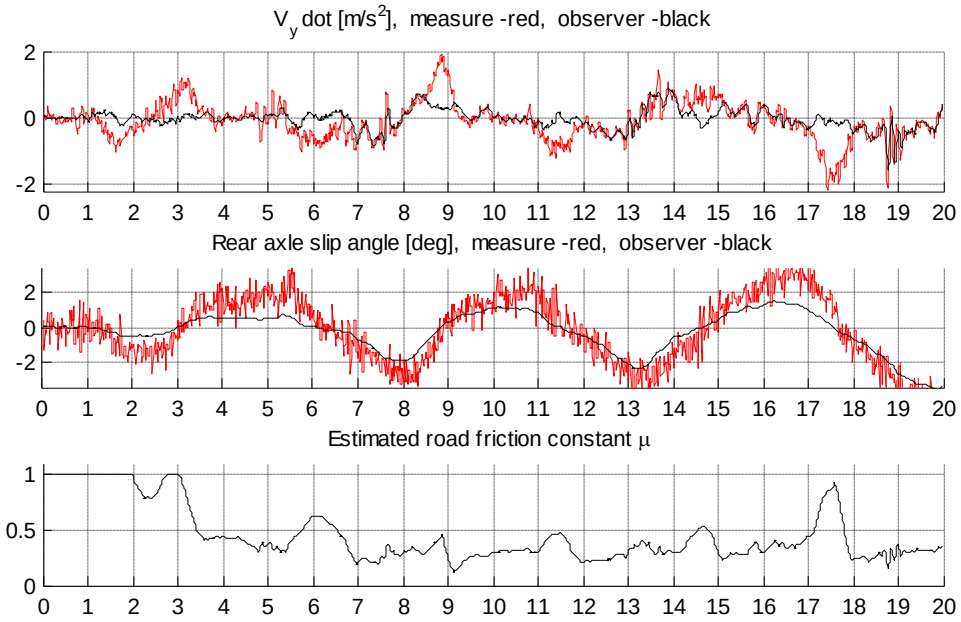

The friction estimation is less accurate in this test. It successfully reduces the friction coefficient in the beginning, but non modeled disturbance prevents it from converging completely.

The friction estimation tends to introduce numerical instabilities, mainly because the noise in the lateral acceleration sensor but also because the risk of self amplification then the friction coefficient is used as feedback.

The problem with noise is possible to be reduced with a low pass filter if one takes the possible phase lag into account.

4.5 Comparison between the Two track model and the Single track model

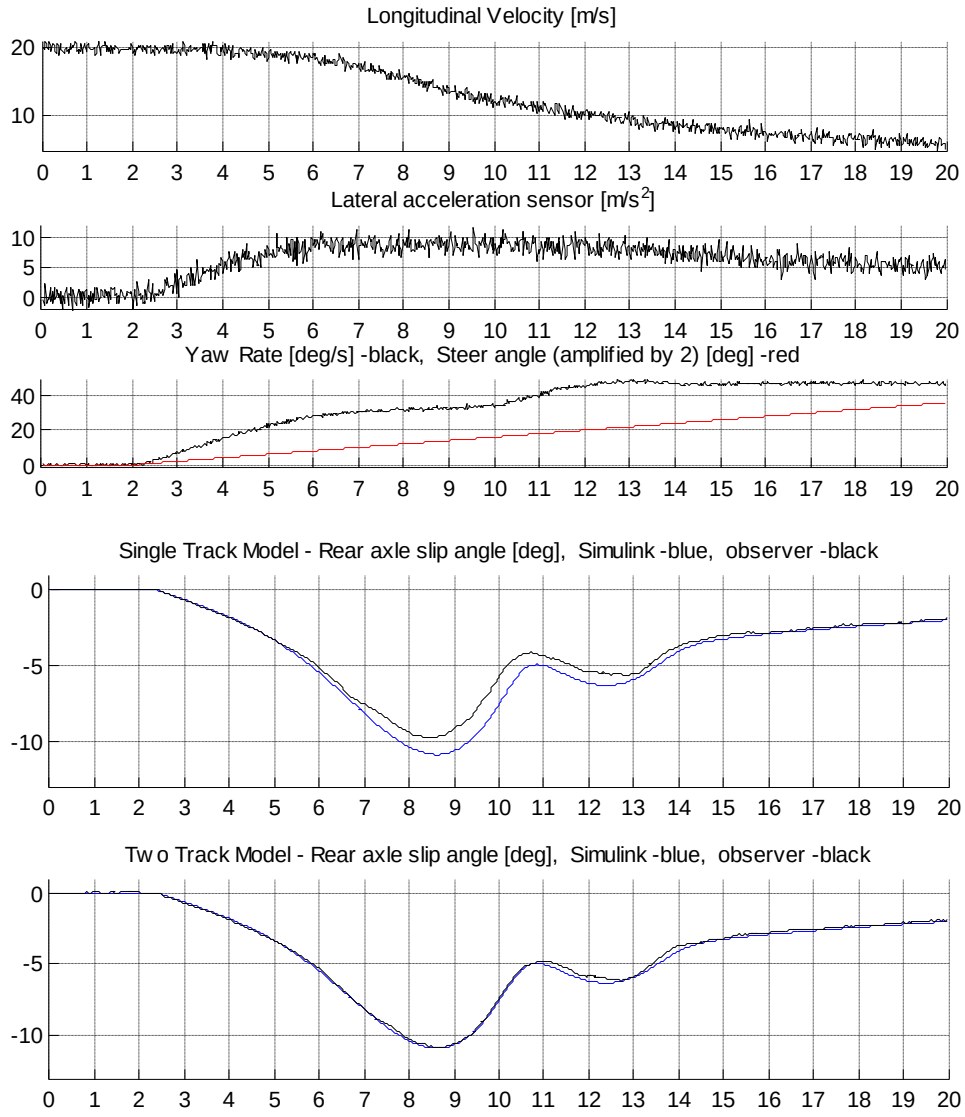

The Single track model captures the slip characteristics quite well, but appears to have a more tire grip. This because the two track model captures load transfer such that the outer wheel pair gets an increasing vertical load and the inner wheel pair gets a decreasing load. If the tire lateral force would have depended linear with respect to the vertical load, there should have been no difference between the two models.
At big lateral accelerations the lateral force doesn't increase at the same rate at the outer wheels as it decrease at the inner wheels.
This non-linearity usually makes difference in the results when the lateral acceleration is bigger than 4-5 m/s^2 [1].

5. Conclusions

5.1 Overview

In the tests against the Simulink model, the results were good. A recurring result was that the observer slide a little more than the Simulink model, probably because the tire model used by the observer was slightly off scaled with the Simulink tire model. In other words, if $\mu_{simulink} = 1$ then the observer has to use e.g. $\mu_{observer} = 1.1$ for best result.
In Test 1.6 with applied torque, the simplified combined slip model delivered good results.

With the experimental data, the results were also good and the observer proved to maintain relatively high accuracy at large slip angles.
In both cases with the experimental data (especially case.1) the tire model used by the observer didn't entirely match the tire used in the experimental tests. This put effort on the observer to try estimating the states using a slightly incorrect tire model.
From the tests it is shown that better results can be achieved if correct tire stiffness factor is used and one could therefore try to find methods to estimate this value as well, Test 2.1a illustrates this best. This value normally only changes at tire wear, tire change and similar, therefore is the rate of convergence in the estimated value allowed to be slow.

The estimation error of the slip angle wasn't able to be reduced with use of the more complex EKF observer, compared to the simpler Averaging Observer.
This indicates that in this setup the estimation accuracy is not limited by the observer complexity.
In reference [1] comparison is made between an EKF observer and a simpler nonlinear observer, the conclusion was also in that work that the change of observer does no particular improvement of the estimation accuracy.

Problems experience then using measurement signals is the influence of unknown offsets and time dependent non linear scaling. The most troublesome measurement signal is from the lateral acceleration sensor which in several cases did more harm to the observer than help.
In general to reduce problems with inaccurate measurements, one should if possible do cross measurements.

The road friction estimation technique based on information of the lateral acceleration sensor proved to work well when evaluated against the Simulink model.
At the case with real world measurements, the road friction estimation did not always converge entirely, mainly because of problems to model the disturbance of the lateral acceleration sensor.

The good results when the road friction coefficient μ were known indicates that if it is possible to estimate the friction coefficient μ well, the observer will have the ability to deliver good estimation of the lateral velocity.

The Two track model was also compared against the simpler Single track model, which confirmed that the Single track model performs well if the lateral acceleration is low, but tends to lose accuracy when the lateral acceleration exceeds $5\ \mathrm{m/s^2}$.
Another advantage of the Two track model is that it should be a better platform to do online estimations of the road friction constant, because the vertical load on each of the four tires is modeled.

5.1 Further work

Because the more complex EKF observer did not improve the results it is suggested to use the simpler Averaging Observer and instead enhance the complexity of the vehicle model. Also there are others observers which may be interesting to look into like Lünenburger and Zeitz.

In all tests were the tunable parameters in both observers kept constant. If there is possible to find good control strategies to adjust these parameters online, better convergent speed and robustness can be achieved.

Tire model
An accurate tire model is the main key to make a good estimation of the lateral velocity.

Most probably are the majority of estimation errors in the tests in this report caused by the fact that the tire model does not completely represent a real world tire.
Optimal it should be able to model combined slip, different downloads and shifting road conditions very well.
The application of this observer, to be able to run real time in a vehicle, puts limitations of the complexity of the tire model. Therefore one may try to develop a tire model that without using too much resource captures most of the tire characteristics as possible.

Road friction estimation
The tire model can not work properly without a correct value of the current road friction coefficient. Because this value changes over time it is necessary to estimate and update it over time.
By use of lateral acceleration sensor, wheel angular velocities, yaw-rate, driveline torque and maybe other signals it should be possible to make cross estimations of the friction coefficient.

Lateral acceleration sensor
Since the lateral acceleration sensor is exposed to disturbances from the chassis, the lateral acceleration signal usually contain quite a bit of noise. The sensor is also subject to offset and scale –errors. If not taken noise and errors into account, the use of the sensor can do more harm than help for the observer.

In the evaluation of the observer against the Simulink source model, much disturbance of the lateral acceleration sensor was on forehand known. When the observer took advantage of this signal it greatly enhanced the speed of convergence and robustness of the estimation of the lateral velocity.

An accurate measurement of the lateral acceleration is also important for good road friction estimation.

In reference [1] the use of the lateral acceleration sensor was limited because the chassis roll motion was not modeled. In this work the chassis roll motion is modeled but still the use of the lateral acceleration sensor is limited due to unknown disturbance.

To make a further step to reduce the disturbance of the lateral acceleration sensor should increase the performance of the observer and also greatly increase the ability to estimate the road friction.

6. References

[1] S.L.G.F.Schoutissen
'Design and Validation of a Vehicle State Estimator' - 2004

[2] Hans B. Pacejka
'Tyre and Vehicle Dynamics' - 2005

[3] Karl Johan Åström
'Computer-controlled systems: theory and design' – 1997

[4] Ahmed A. Shabana
'Dynamics of Multibody Systems' - 1998

7. List of Symbols

α	Tire lateral slip angle - [*rad*]
a_x	Longitudinal acceleration - [m/s^2]
a_y	Lateral acceleration - [m/s^2]
β	Chassis slip angle - [*rad*]
β_{rear}	Chassis rear axle slip angle - [*rad*]
δ	Wheel steer angle - [*rad*]
d_L	Length from center of gravity to left wheels - [m]
d_R	Length from center of gravity to right wheels - [m]
F_c	Centripetal force - [*N*]
F_x	Tire longitudinal force - [*N*]
F_y	Tire lateral force - [*N*]
F_z	Tire normal force - [*N*]
g	Gravity acceleration constant
I_{xx}	Moment of inertia with respect of x-axis - [kgm^2]
I_{yy}	Moment of inertia with respect of y-axis - [kgm^2]
I_{zz}	Moment of inertia with respect of z-axis - [kgm^2]
κ	Tire longitudinal slip angle
L_F	Length from center of gravity to front wheels - [m]
L_R	Length from center of gravity to rear wheels - [m]
M_x	Resulting tire momentum around x-axis - [Nm]
M_y	Resulting tire momentum around y-axis - [Nm]
M_z	Resulting tire momentum around z-axis - [Nm]
m	Vehicle mass - [kg]
v_{CoG}	Velocity vector of chassis center of gravity - [m/s]
v_x	Chassis longitudinal velocity - [m/s]
v_y	Chassis lateral velocity - [m/s]
ϕ	Chassis roll angle - [*rad*]
θ	Chassis pitch angle - [*rad*]
ψ	Chassis yaw angle - [*rad*]
μ	Tire road friction coefficient
ϖ	Wheel angular velocity - [rad/s]